nature portfolio

https://doi.org/10.1038/s41565-021-00950-z

Supplementary information

Immunogenic camptothesome nanovesicles comprising sphingomyelin-derived camptothecin bilayers for safe and synergistic cancer immunochemotherapy

In the format provided by the authors and unedited

Supplemental Information

Immunogenic Camptothesome Nanovesicles Comprised by Sphingomyelin-derived Camptothecin Bilayers for Safe and Synergistic Cancer Immunochemotherapy

Zhiren Wang[1], Nicholas Little[1], Jiawei Chen[1], Kevin Tyler Lambesis[1], Kimberly Thi Le[1], Weiguo Han[1], Aaron James Scott[2,3], Jianqin Lu[1,2,4,5]*

[1]Skaggs Pharmaceutical Sciences Center, Department of Pharmacology & Toxicology, College of Pharmacy, The University of Arizona, Tucson, Arizona, 85721, United States

[2]NCI-designated University of Arizona Comprehensive Cancer Center, Tucson, Arizona, 85721, United States

[3]Division of Hematology and Oncology, Department of Medicine, College of Medicine, The University of Arizona, Tucson, Arizona, 85721, United States

[4]BIO5 Institute, The University of Arizona, Tucson, Arizona, 85721, United States

[5]Southwest Environmental Health Sciences Center, The University of Arizona, Tucson, 85721, United States

Materials

(S)-(+)-camptothecin (CPT, 98%), 1-methyl-D-tryptophan (IND, 98%), Doxorubicin hydrochloride (DOX, 98%), Di(1*H*-imidazol-1-yl)methanone (CDI, 98%), O-(7-Azabenzotriazol-1-yl)-N,N,N,N-tetramethyl uronium hexafluorophosphate (HATU, 98%), 2,3,4,6,7,8,9,10-Octahydropyrimido[1,2-*a*]azepine (DBU, 98%), and (tert-butoxycarbonyl)glycine (98%) were purchased from BLDpharm (Shanghai, China). Sphingomyelin (egg, 99%), DSPE-PEG_{2K} (99%), DSPE-PEG_{2K}-Folate (99%), DSPE-Cy5.5 (99%), and cholesterol (ovine, 99%) were purchased from Avanti (Alabama, USA). Succinic anhydride (98%), N, N-diisopropylethylamine (98%), 4-Dimethylaminopyridine (DMAP, 98%), triphosgene (98%), 4-pyrrolidinopyridine (4-PPY, 98%), and EDCI (98%), Di-*tert*-butyl decarbonate (98%) were purchased from Fisher Scientific (USA). 2, 2'-dithiodiethanol (98%) was purchased from Sigma-Aldrich (MO, USA). Doxil and Onivyde were acquired from Pharmacy Department, Banner-University Medical Center Tucson. Trypsin-EDTA solution, Triton X-100, and Dulbecco's Modified Eagle's Medium (DMEM), RPMI-1640 medium, fetal bovine serum (FBS), and penicillin-streptomycin solution were all purchased from Gibco (MD, USA). All solvents used for chemical reactions were anhydrous, and the eluting solvents for compound purification were HPLC grade.

Chemical synthesis

The NMR spectra were acquired by VNMRJ software (v. 4.2) using TMS (0 ppm) as the internal standard on a Varian 400 MHz spectrometer and analysed by MestReNova (v. 6.0.2). ^{1}H NMR data were reported as follows: chemical shift, multiplicity (s = singlet, d = doublet,

m = multiplet), coupling constant in Hertz (Hz) and hydrogen numbers based on integration intensities. ^{13}C NMR chemical shifts are reported in ppm relative to the central peak of TMS (0 ppm) as internal standards. The high-resolution mass spectra (HRMS) were generated via a LTQ Orbitrap Velos mass spectrometer with an ESI source (Thermo Scientific). The low-resolution mass spectra were generated using a LCMS-2020 + DUIS-2020 (Shimadzu). The reactions were followed by thin-layer chromatography (TLC, Silica gel 60 F_{254}, Merck KGaA) on glass-packed precoated silica gel plates and visualized in an iodine chamber or with a UV lamp. Flash column chromatography was performed using silica gel (SiliaFlash® P60, 230–400 mesh) purchased from Silicycle Inc.

The synthesis of SM-Ester-CPT.

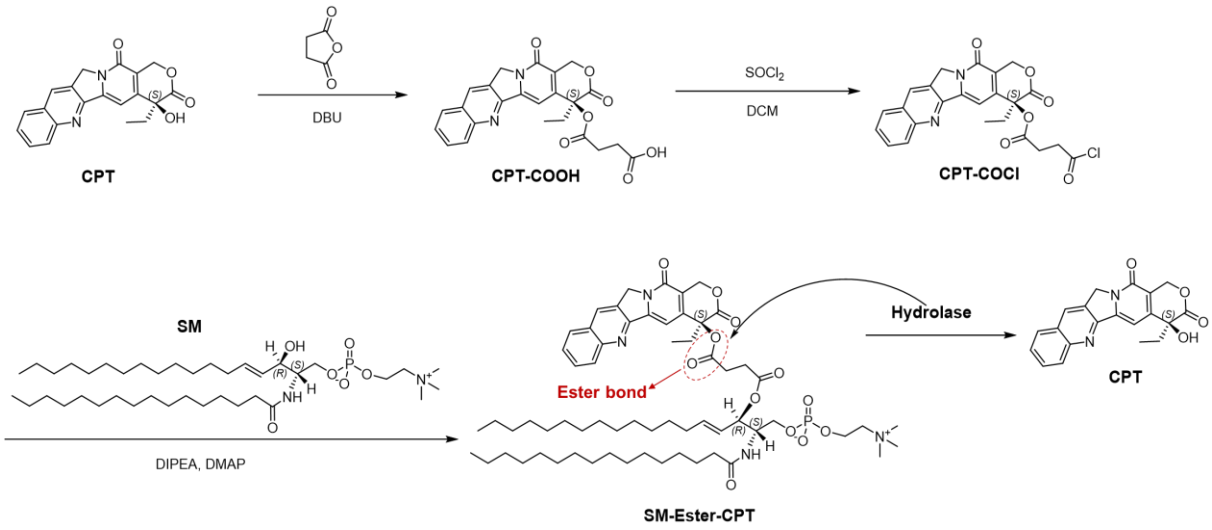

Supplementary Scheme 1, Synthetic route for SM-derived CPT with ester bond (SM-Ester-CPT).

(*S*)-4-((4-ethyl-3,14-dioxo-3,4,12,14-tetrahydro-1*H*-pyrano[3′,4′:6,7]indolizino[1,2-*b*]quinolin-4-yl)oxy)-4-oxobutanoic acid (CPT-COOH)[1].

1,8-diazabicycloundec-7-ene (DBU, 46 mL, 30 mmol) was added dropwise at 0 °C to a solution of (*S*)-(+)-camptothecin (3.48 g, 10 mmol) and succinic anhydride (3.0 g, 30 mmol) in 100 mL of anhydrous dichloromethane (DCM). The reaction was further stirred at room temperature for 3 h and monitored by TLC. After the completion of the reaction, the solution was acidified to pH = 2.0 by HCl aqueous solution (10%), and then filtrated. The collected pellet was dried under reduced pressure to yellow solid product and used for the next step without further purification. Yellow solid with 96% yield was attained. R_f = 0.32 (CH_2Cl_2/CH_3OH = 20/1). ^{1}H NMR (400 MHz, DMSO-d_6) δ 8.65 (s, 1H), 8.14 (d, *J* = 8.5 Hz, 1H), 8.09 (d, *J* = 8.1 Hz, 1H), 7.83 (dd, *J* = 11.3, 4.1 Hz, 1H), 7.68 (t, *J* = 7.2 Hz, 1H), 7.09 (s, 1H), 5.53 – 5.38 (m, 2H), 5.34 – 5.18 (m, 2H), 2.73 (ddt, *J* = 30.7, 17.8, 6.7 Hz, 2H), 2.12 (dd, *J* = 14.7, 7.2 Hz, 2H), 1.58 (s, 1H), 0.88 (t, *J* = 7.3 Hz, 3H). ^{13}C NMR (101 MHz, DMSO-d_6) δ 173.39, 171.68, 167.58, 156.94, 152.79, 148.30, 146.33, 145.67, 131.95, 130.80, 130.18, 129.42, 128.93, 128.37, 128.11, 119.33, 95.54, 76.30, 66.72, 50.61, 30.82, 28.99, 28.80, 7.96. LC/MS (ESI): 449.1 $[M + H]^+$.

(*S*)-4-ethyl-3,14-dioxo-3,4,12,14-tetrahydro-1*H*-pyrano[3',4':6,7]indolizino[1,2-*b*]quinolin-4-yl 4-chloro-4-oxobutanoate (CPT-COCl).

Thionyl chloride (3 mL) was added to a solution of intermediate product CPT-COOH (1.0 g, 2.1 mmol) in 20 mL anhydrous DCM at 0 °C. The reaction was stirred at room temperature and monitored by the TLC. After the completion of the reaction, the solvent was evaporated under vacuum, the product was used for the next step directly without any further purification.

(2*S*,3*R*,*E*)-3-((4-(((*S*)-4-ethyl-3,14-dioxo-3,4,12,14-tetrahydro-1*H*-pyrano[3',4':6,7]indolizino[1,2-*b*]quinolin-4-yl)oxy)-4-oxobutanoyl)oxy)-2-palmitamidooctadec-4-en-1-yl (2-(trimethylammonio)ethyl) phosphate (**SM-Ester-CPT**).

N, *N*-diisopropylethylamine (258.5 mg, 2.0 mmol) and DMAP (12.2 mg, 0.1 mmol) was added to a solution of sphingomyelin (703.0 mg, 1.0 mmol) in anhydrous DCM (30 mL). The mixture solution was stirred at 0 °C with a dropwise addition of a solution of CPT-COCl (932.2 mg, 2.0 mmol) in 10 mL anhydrous DCM. The reaction was stirred at room temperature for 48 h and monitored by TLC. The solvent was then removed under reduced pressure, the product was extracted by DCM (50 mL × 5). The organic phase was washed with saturated brine, dried with anhydrous Na_2SO_4, and the solvent was evaporated using rotary evaporator (RV 10 digital, IKA®) under vacuum followed by purification by silica gel flash chromatography with $CHCl_3$/EtOH/H_2O (v/v/v, 300/200/36) as the eluting solvent. Yellow solid with 42% yield was obtained. R_f = 0.28 ($CHCl_3$/EtOH/H_2O = 300/200/36). ^{1}H NMR (400 MHz, $CDCl_3$) δ 8.36 (s, 1H), 8.19 (d, *J* = 8.4 Hz, 1H), 7.89 (d, *J* = 7.9 Hz, 1H), 7.83 – 7.78 (m, 1H), 7.65 – 7.60 (m, 1H), 7.53 (s, 1H), 7.14 (s, 1H), 5.62 (d, *J* = 16.7 Hz, 2H), 5.37 – 5.24 (m, 4H), 4.24 (s, 2H), 4.17 (s, 1H), 3.83 (s, 2H), 3.68 (d, *J* = 17.9 Hz, 3H), 3.27 (s, 9H), 2.92 – 2.85 (m, 1H), 2.76 – 2.69 (m, 1H), 2.61 (dd, *J* = 14.7, 3.3 Hz, 1H), 2.51 – 2.43 (m, 1H), 2.23 (dd, *J* = 13.8, 7.3 Hz, 1H), 2.15 – 2.10 (m, 1H), 2.05 (s, 2H), 1.86 (d, *J* = 5.1 Hz, 2H), 1.46 (s, 2H), 1.20 (d, *J* = 11.3 Hz, 46H), 0.94 (t, *J* = 7.1 Hz, 3H), 0.84 (t, *J* = 5.9 Hz, 6H).^{13}C NMR (101 MHz, $CDCl_3$) δ 173.12, 171.61, 170.78, 167.70, 157.15, 152.13, 148.76, 146.58, 145.43, 137.64, 131.25, 130.66, 129.59, 128.55, 128.17, 128.01, 125.03, 119.82, 95.54, 76.06, 74.21, 67.10, 66.28, 66.26, 63.85, 63.81, 59.31, 59.27, 54.50, 50.90, 50.04, 36.66, 32.23, 31.89, 31.68, 29.70, 29.64,

29.59, 29.54, 29.50, 29.40, 29.33, 28.91, 28.68, 28.30, 25.78, 22.65, 14.09, 7.54. HRMS (ESI) m/z $[M + Na]^+$ for $C_{63}H_{97}N_4O_{12}P$ calculated 1155.6733, found 1155.6772; HPLC retention time: 10.260 min.

The synthesis of SM-SS-CPT.

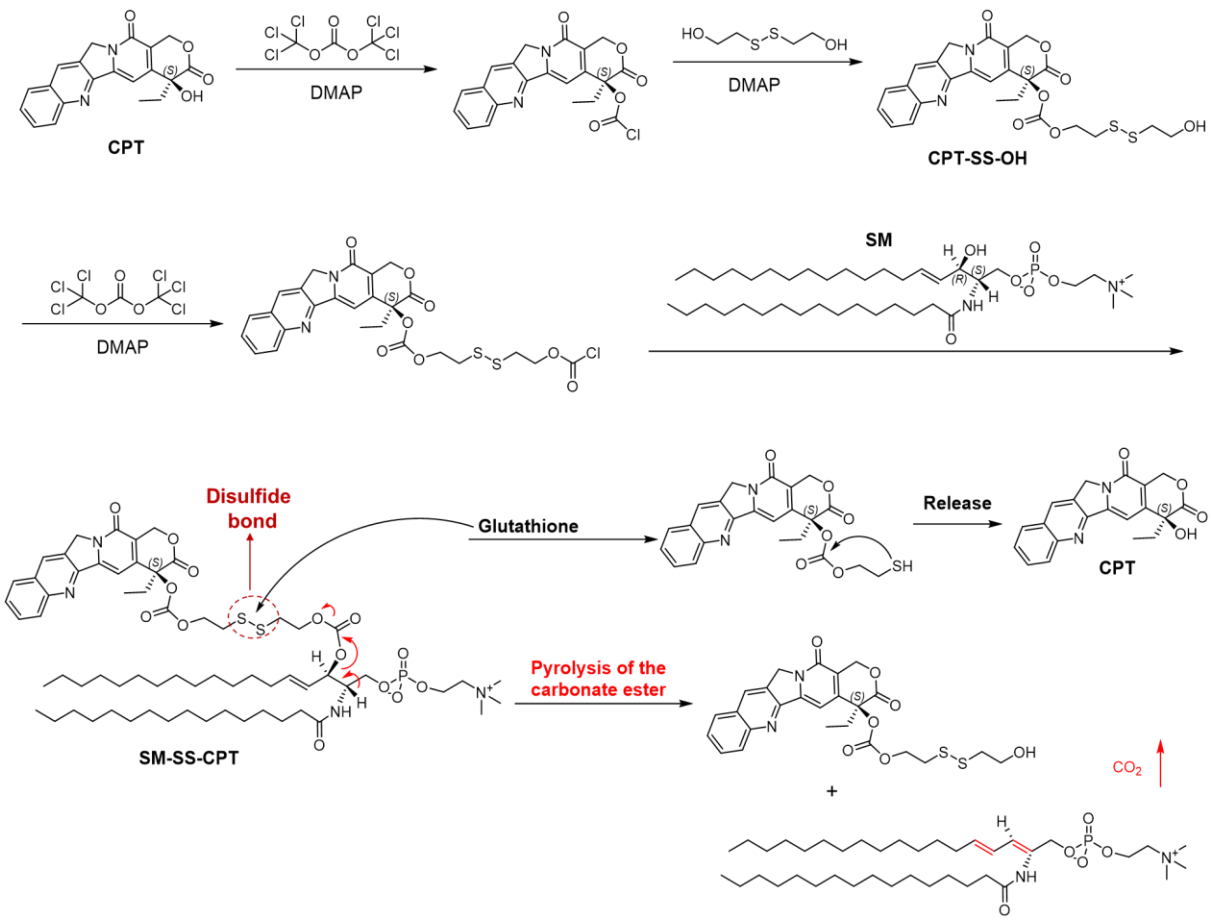

Supplementary Scheme 2, Synthetic route for SM-derived CPT with disulfide bond (SM-SS-CPT).

(*S*)-4-ethyl-3,14-dioxo-3,4,12,14-tetrahydro-1*H*-pyrano[3',4':6,7]indolizino[1,2-*b*]quinolin-4-yl (2-((2-hydroxyethyl)disulfanyl)ethyl) carbonate (CPT-SS-OH)[2].

DMAP (3.67 g, 30 mmol, in 15 mL anhydrous DCM) was added dropwise to a solution of (*S*)-(+)-camptothecin (3.48 g, 10 mmol) and triphosgene (1.03 g, 3.4 mmol) in anhydrous DCM (150 mL). The reaction was stirred at room temperature for 30 min, then a solution of 2, 2'-dithiodiethanol (9.25 g, 60 mmol) in anhydrous THF (25 mL) was added into the mixture solution. The reaction was further stirred at room temperature for 12 h and monitored by TLC. After completion of the reaction, the mixture solution was washed with 50 mM HCl aqueous solution to remove the DMAP, and then with saturated brine. The organic layer was dried with anhydrous Na_2SO_4, the solvent was evaporated using rotary evaporator under vacuum, and the residue was purified by silica gel flash chromatography. Yellow solid with 71% yield was acquired. R_f = 0.38 (CH_2Cl_2/CH_3OH = 20/1). ^{1}H NMR (400 MHz, $CDCl_3$) δ 8.41 (s, 1H), 8.20 (t, *J* = 11.2 Hz, 1H), 7.94 (d, *J* = 8.1 Hz, 1H), 7.84 (t, *J* = 7.2 Hz, 1H), 7.67 (t, *J* = 7.1 Hz, 1H), 7.42 (s, 1H), 5.70 (d, *J* = 17.3 Hz, 1H), 5.38 (d, *J* = 17.3 Hz, 1H), 5.29 (s, 2H), 4.45 – 4.25 (m, 2H), 3.89 (pd, *J* = 11.8, 6.2 Hz, 2H), 3.27 (t, *J* = 5.9 Hz, 1H), 3.05 – 2.78 (m, 4H), 2.28 (td, *J* = 14.9, 7.5 Hz, 1H), 2.15 (td, *J* = 15.0, 7.6 Hz, 1H), 1.00 (t, *J* = 7.5 Hz, 3H). ^{13}C NMR (101 MHz, DMSO-d_6) δ 167.47, 156.90, 153.21, 152.62, 148.29, 146.66, 145.14, 132.02, 130.86, 130.20, 129.41, 128.94, 128.43, 128.17, 119.60, 94.79, 78.30, 66.87, 66.73, 59.71, 50.75, 41.53, 36.60, 30.74, 7.99. LC/MS (ESI): 529.1 $[M + H]^+$.

(12*R*,13*S*)-1-(((*S*)-4-ethyl-3,14-dioxo-3,4,12,14-tetrahydro-1*H*-pyrano[3',4':6,7]indolizino[1,2-*b*]quinolin-4-yl)oxy)-1,10-dioxo-13-palmitamido-12-((*E*)-pentadec-1-en-1-yl)-2,9,11-trioxa-5,6-dithiatetradecan-14-yl (2-(trimethylammonio)ethyl) phosphate (SM-SS-CPT).

DMAP (367 mg, 3 mmol, in 5 mL anhydrous DCM) was added dropwise to a solution of CPT-SS-OH (528 mg, 1.0 mmol) and triphosgene (103 mg, 0.34 mmol) in anhydrous DCM (100 mL). The reaction mixture was stirred at room temperature for 20 min. Then sphingomyelin (703.0 mg, 1.0 mmol) was added into the mixture solution. The reaction was further stirred at room temperature for 12 h and monitored by TLC. After completion of the reaction, the mixture solution was washed with 50 mM HCl aqueous solution to remove the DMAP, and then with saturated brine. The organic layer was dried with anhydrous Na_2SO_4, the solvent was evaporated using rotary evaporator under vacuum, and the residue was purified by silica gel flash chromatography with $CHCl_3$/EtOH/H_2O (v/v/v, 300/200/36) as the eluting solvent. Yellow solid with 56% yield was obtained. R_f = 0.31 ($CHCl_3$/EtOH/H_2O = 300/200/36). ^{1}H NMR (400 MHz, $CDCl_3$) δ 8.43 (s, 1H), 8.22 (d, *J* = 8.5 Hz, 1H), 7.95 (d, *J* = 8.1 Hz, 1H), 7.87 – 7.82 (m, 1H), 7.70 – 7.65 (m, 1H), 7.61 (d, *J* = 8.3 Hz, 1H), 7.32 (s, 1H), 5.76 (dd, *J* = 14.8, 7.6 Hz, 1H), 5.70 (d, *J* = 17.2 Hz, 1H), 5.48 – 5.42 (m, 1H), 5.39 (d, *J* = 17.1 Hz, 1H), 5.31 (s, 2H), 5.15 (t, *J* = 8.1 Hz, 1H), 4.45 – 4.31 (m, 4H), 4.29 – 4.23 (m, 2H), 3.97 (d, *J* = 5.6 Hz, 2H), 3.83 (dt, *J* = 35.0, 13.3 Hz, 3H), 3.35 (s, 9H), 2.95 (t, *J* = 6.2 Hz, 2H), 2.88 (dd, *J* = 7.2, 5.5 Hz, 2H), 2.31 (s, 2H), 2.17 – 2.12 (m, 2H), 2.01 – 1.93 (m, 2H), 1.54 (s, 2H), 1.25 (t, *J* = 12.5 Hz, 46H), 1.01 (t, *J* = 7.4 Hz, 3H), 0.87 (t, *J* = 6.7 Hz, 6H). ^{13}C NMR (101 MHz, $CDCl_3$) δ 173.33, 167.51, 157.19, 153.94, 153.44, 152.17, 148.85, 146.63, 145.47, 138.23, 131.24, 130.72, 129.63, 128.47, 128.19, 128.10, 124.38, 119.94, 95.82, 78.12, 78.06, 77.18, 67.09, 66.51, 66.36, 65.21, 63.76, 59.25, 54.65, 51.27, 50.07, 37.06, 36.77, 36.71, 32.31, 31.89, 31.76, 29.71, 29.70, 29.65, 29.60, 29.56, 29.51, 29.40, 29.34, 28.91, 25.79, 22.66, 14.09, 7.64.

HRMS (ESI) m/z $[M + H]^+$ for $C_{65}H_{102}N_4O_{14}PS_2$ calculated 1257.6566, found 1257.6594; HPLC retention time: 13.371 min.

The synthesis of SM-Glycine-CPT.

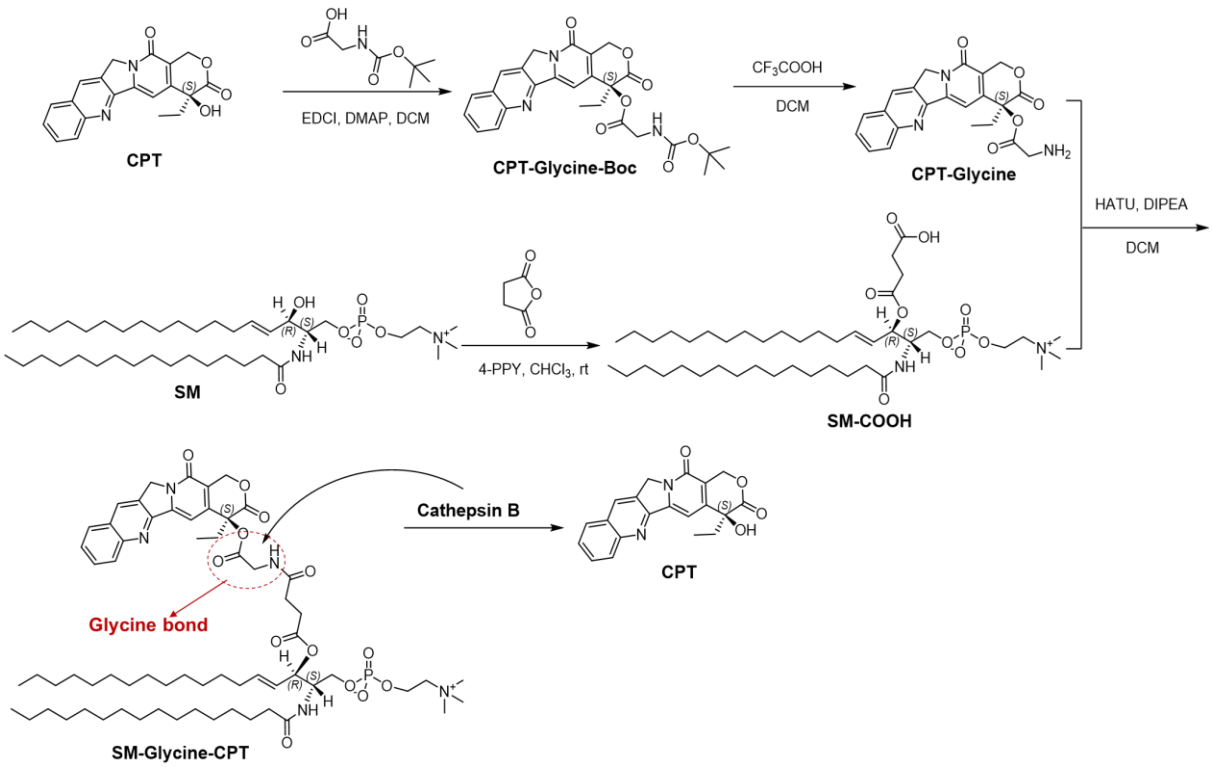

Supplementary Scheme 3, Synthetic route for SM-derived CPT with glycine bond (SM-Glycine-CPT).

(2*S*,3*R*,*E*)-3-((3-carboxypropanoyl)oxy)-2-palmitamidooctadec-4-en-1-yl (2-(trimethylammonio)ethyl) phosphate (SM-COOH).

4-pyrrolidinopyridine (4-PPY, 44.4 mg, 0.3 mmol) was added to a solution of sphingomyelin (2.1 g, 3.0 mmol) and succinic anhydride (3 g, 30 mmol) in anhydrous $CHCl_3$ (100 mL). The solution was stirred at room temperature for 12 h and monitored by TLC. After completion of

the reaction, CH_3OH (30 mL) was added into the mixture solution, the reaction was further stirred at room temperature for 12 h. The solvent was evaporated using rotary evaporator under vacuum, and the residue was purified by silica gel flash chromatography with $CHCl_3$/EtOH/H_2O (v/v/v, 300/200/36) as the elution solvent. White solid with 93% yield was garnered. R_f = 0.23 ($CHCl_3$/EtOH/H_2O = 300/200/36). ^{1}H NMR (400 MHz, $CDCl_3$) δ 6.98 (d, *J* = 6.7 Hz, 1H), 5.75 – 5.68 (m, 1H), 5.39 (dd, *J* = 15.0, 8.3 Hz, 1H), 5.28 (t, *J* = 8.8 Hz, 1H), 4.29 (d, *J* = 4.4 Hz, 3H), 3.94 (s, 2H), 3.77 (s, 2H), 3.28 (s, 9H), 2.64 (dd, *J* = 13.1, 6.3 Hz, 2H), 2.39 (dd, *J* = 14.3, 6.6 Hz, 2H), 2.12 (q, *J* = 13.9 Hz, 2H), 1.97 (d, *J* = 6.6 Hz, 2H), 1.55 (s, 2H), 1.28 (d, *J* = 19.0 Hz, 46H), 0.88 (t, *J* = 6.7 Hz, 6H). ^{13}C NMR (101 MHz, $CDCl_3$) δ 174.74, 173.10, 172.06, 137.75, 125.20, 73.28, 65.76, 65.70, 64.26, 64.23, 59.20, 59.15, 54.32, 50.66, 50.61, 36.66, 32.25, 31.88, 29.74, 29.71, 29.70, 29.69, 29.63, 29.60, 29.56, 29.50, 29.46, 29.33, 28.92, 25.79, 22.64, 14.06. HRMS (ESI) m/z $[M + H]^+$ for $C_{43}H_{84}N_2O_9P$ calculated 803.5909, found 803.5928.

(*S*)-4-ethyl-3,14-dioxo-3,4,12,14-tetrahydro-1*H*-pyrano[3',4':6,7]indolizino[1,2-*b*]quinolin-4-yl (tert-butoxycarbonyl)glycinate (CPT-Glycine-Boc).

EDCI (2.10g, 11.0 mmol) and 2 mL DIPEA was added to a solution of (*tert*-butoxycarbonyl)glycine (1.75g, 10.0 mmol) in 100 mL anhydrous DCM followed by stirring at room temperature for 30 min. (*S*)-(+)-camptothecin (3.48 g, 10 mmol) and DMAP (122 mg, 1.0 mmol) was then added into the mixture solution. The reaction was further stirred at room temperature for 12 h and monitored by TLC. After completion of the reaction, the mixture solution was washed with 50 mM HCl aqueous solution to remove the DMAP, and then with saturated brine. The organic layer was dried with anhydrous Na_2SO_4, the solvent was

evaporated using rotary evaporator under vacuum, and the residue was purified by silica gel flash chromatography. Yellow solid with 96% yield was gained. R_f = 0.43 (petroleum/EtOAc = 1/1). ^{1}H NMR (400 MHz, $CDCl_3$) δ 8.39 (s, 1H), 8.24 (d, *J* = 8.2 Hz, 1H), 7.94 (d, *J* = 8.1 Hz, 1H), 7.84 (t, *J* = 7.5 Hz, 1H), 7.67 (t, *J* = 7.4 Hz, 1H), 7.27 (d, *J* = 6.1 Hz, 1H), 5.69 (d, *J* = 17.2 Hz, 1H), 5.41 (d, *J* = 17.2 Hz, 1H), 5.29 (d, *J* = 6.3 Hz, 2H), 4.97 (s, 1H), 4.20 (dd, *J* = 18.2, 5.9 Hz, 1H), 4.07 (dd, *J* = 18.1, 4.7 Hz, 1H), 2.30 (td, *J* = 14.8, 7.4 Hz, 1H), 2.17 (td, *J* = 14.8, 7.4 Hz, 1H), 1.77 (s, 1H), 1.53 – 1.24 (m, 9H), 0.99 (t, *J* = 7.4 Hz, 3H). ^{13}C NMR (101 MHz, $CDCl_3$) δ 169.49, 167.13, 157.28, 155.42, 152.22, 148.86, 146.40, 145.39, 131.05, 130.58, 129.73, 128.35, 128.12, 127.99, 120.10, 96.17, 80.13, 77.18, 76.75, 67.09, 49.93, 42.39, 31.75, 28.22, 7.53. LC/MS (ESI): 506.1 $[M + H]^+$.

(*S*)-4-ethyl-3,14-dioxo-3,4,12,14-tetrahydro-1*H*-pyrano[3',4':6,7]indolizino[1,2-*b*]quinolin-4-yl glycinate (CPT-Glycine).

CF_3COOH (1 mL) was added to a solution of CPT-Glycine-Boc (505 mg, 1.0 mmol) in anhydrous DCM (50 mL) in an ice bath. The reaction was stirred at room temperature for 0.5 h and monitored by TLC. After completion of the reaction, the solvent was evaporated using rotary evaporator under vacuum. This intermediate was used for the next step immediately without further purification.

(2*S*,3*R*,*E*)-3-((4-((2-(((*S*)-4-ethyl-3,14-dioxo-3,4,12,14-tetrahydro-1*H*-pyrano[3',4':6,7]indolizino[1,2-*b*]quinolin-4-yl)oxy)-2-oxoethyl)amino)-4-oxobutanoyl)oxy)-2-palmitamidooctadec-4-en-1-yl (2-(trimethylammonio)ethyl) phosphate (SM-Glycine-CPT).

DIPEA (2 mL) was added to a solution of SM-COOH (803.0 mg, 1.0 mmol) and HATU (380 mg, 1.0 mmol) in anhydrous DCM (50 mL). The reaction mixture was stirred at room temperature for 30 min. A solution of CPT-Glycine (1.0 mmol) in 10 mL anhydrous DCM was added into the reaction and further stirred for 12 h. After completion of the reaction, the reaction mixture was washed with 50 mM HCl aqueous solution, and then with saturated brine. The organic layer was dried with anhydrous Na_2SO_4, the solvent was removed using rotary evaporator under vacuum, and the residue was purified by silica gel flash chromatography with $CHCl_3$/EtOH/H_2O (v/v/v, 300/200/36) as the eluting solvent. Pale yellow solid with 78% yield was achieved. R_f = 0.32 ($CHCl_3$/EtOH/H_2O = 300/200/36). ^{1}H NMR (400 MHz, $CDCl_3$) δ 8.60 (s, 1H), 8.36 (s, 1H), 8.21 (d, *J* = 8.5 Hz, 1H), 7.90 (d, *J* = 8.1 Hz, 1H), 7.82 – 7.77 (m, 1H), 7.66 – 7.60 (m, 1H), 7.29 (s, 1H), 7.14 (d, *J* = 8.1 Hz, 1H), 5.69 – 5.59 (m, 2H), 5.39 – 5.19 (m, 5H), 4.36 (dd, *J* = 18.0, 5.7 Hz, 1H), 4.23 (s, 2H), 4.13 (s, 1H), 4.01 (dd, *J* = 17.9, 4.3 Hz, 1H), 3.86 – 3.76 (m, 2H), 3.67 (s, 2H), 3.25 (s, 9H), 2.56 (s, 4H), 2.24 (dd, *J* = 14.0, 7.3 Hz, 1H), 2.17 – 2.13 (m, 1H), 2.12 – 2.05 (m, 2H), 1.88 (d, *J* = 6.4 Hz, 2H), 1.50 (s, 2H), 1.21 (d, *J* = 10.2 Hz, 46H), 0.93 (t, *J* = 7.3 Hz, 3H), 0.86 (t, *J* = 6.6 Hz, 6H). ^{13}C NMR (101 MHz, $CDCl_3$) δ 173.31, 172.53, 171.97, 169.91, 167.85, 157.16, 152.01, 148.69, 146.52, 145.38, 137.06, 131.19, 130.56, 129.69, 128.42, 128.10, 127.98, 124.65, 119.54, 96.31, 76.46, 73.54, 67.15, 66.28, 66.21, 64.17, 59.25, 59.20, 54.29, 51.11, 51.06, 50.02, 41.00, 36.57, 32.30, 31.90, 31.62, 30.38, 29.93, 29.72, 29.65, 29.61, 29.56, 29.52, 29.39, 29.35, 28.93, 25.86, 22.66, 14.10, 7.53. HRMS (ESI) m/z $[M + H]^+$ for $C_{65}H_{101}N_5O_{13}P$ calculated 1190.7128, found 1190.7169; HPLC retention time: 10.801 min.

The synthesis of SM-CSS-CPT.

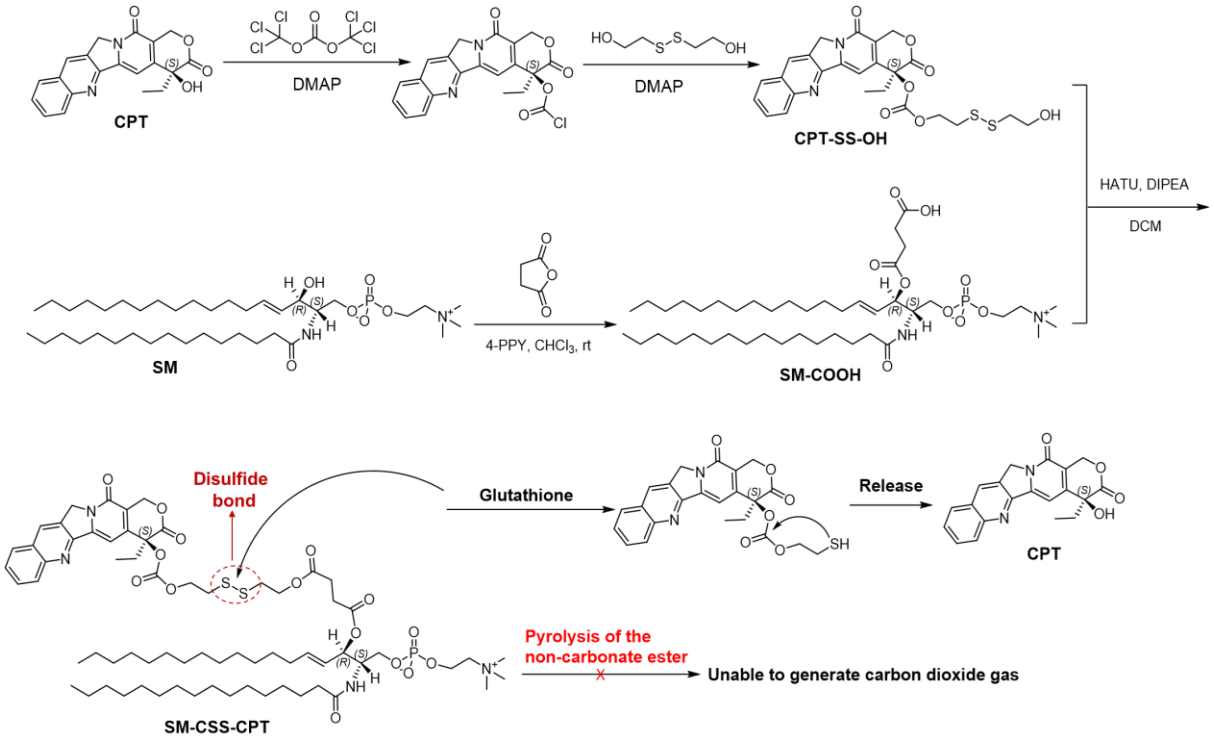

Supplementary Scheme 4, Synthetic route for SM-derived CPT with disulfide bond and longer linker (SM-CSS-CPT).

(15*R*,16*S*)-1-(((*S*)-4-ethyl-3,14-dioxo-3,4,12,14-tetrahydro-1*H*-pyrano[3',4':6,7]indolizino[1,2-*b*]quinolin-4-yl)oxy)-1,10,13-trioxo-16-palmitamido-15-((*E*)-pentadec-1-en-1-yl)-2,9,14-trioxa-5,6-dithiaheptadecan-17-yl (2-(trimethylammonio)ethyl) phosphate (SM-CSS-CPT).

DIPEA (2 mL) was added to a solution of SM-COOH (803.0 mg, 1.0 mmol) and HATU (380 mg, 1.0 mmol) in anhydrous DCM (50 mL). The solution mixture was stirred at room temperature for 30 min. A solution of CPT-SS-OH (528 mg, 1.0 mmol) in 10 mL anhydrous DCM was then added into the reaction mixture and further stirred for 12 h. After completion of the reaction, the reaction mixture was washed with 50 mM HCl aqueous solution and then with saturated brine. The organic layer was dried with anhydrous Na_2SO_4, the solvent was

evaporated using rotary evaporator under vacuum, and the residue was purified by silica gel flash chromatography with $CHCl_3$/EtOH/H_2O (v/v/v, 300/200/36) as the eluting solvent. Pale yellow solid with78% yield was attained. R_f = 0.30 ($CHCl_3$/EtOH/H_2O = 300/200/36). ^{1}H NMR (400 MHz, $CDCl_3$) δ 8.43 (s, 1H), 8.22 (d, *J* = 8.5 Hz, 1H), 7.96 (d, *J* = 8.1 Hz, 1H), 7.85 (t, *J* = 7.6 Hz, 1H), 7.68 (t, *J* = 7.5 Hz, 1H), 7.39 (d, *J* = 8.8 Hz, 1H), 7.32 (s, 1H), 5.74 – 5.67 (m, 2H), 5.44 – 5.31 (m, 5H), 4.38 (dt, *J* = 11.7, 4.9 Hz, 4H), 4.30 – 4.22 (m, 3H), 4.01 – 3.87 (m, 2H), 3.85 – 3.71 (m, 2H), 3.34 (s, 9H), 2.94 (t, *J* = 6.4 Hz, 2H), 2.87 (t, *J* = 6.3 Hz, 2H), 2.62 – 2.51 (m, 4H), 2.36 – 2.09 (m, 3H), 1.96 (d, *J* = 6.9 Hz, 3H), 1.54 (s, 2H), 1.24 (d, *J* = 3.9 Hz, 46H), 1.01 (t, *J* = 7.4 Hz, 3H), 0.87 (t, *J* = 6.6 Hz, 6H). ^{13}C NMR (101 MHz, $CDCl_3$) δ 173.24, 172.16, 171.17, 167.37, 157.21, 153.43, 152.21, 148.85, 146.57, 145.49, 137.45, 131.25, 130.72, 129.61, 128.48, 128.22, 128.19, 128.10, 124.81, 120.05, 95.82, 78.05, 77.18, 74.18, 67.07, 66.59, 66.53, 66.46, 63.90, 63.86, 62.36, 59.25, 59.20, 54.66, 51.17, 51.13, 50.05, 37.08, 36.81, 36.65, 32.30, 31.89, 31.81, 29.70, 29.64, 29.59, 29.52, 29.41, 29.34, 28.98, 28.88, 25.82, 22.66, 14.09, 7.63. HRMS (ESI) m/z $[M + H]^+$ for $C_{68}H_{106}N_4O_{15}PS_2$ calculated 1313.6828, found 1313.6872; HPLC retention time: 13.074 min.

The synthesis of DOX-IND.

***N*$^{\alpha}$-(tert-butoxycarbonyl)-1-methyl-*D*-tryptophan (Boc-IND)[3].**

$NaHCO_3$ (2.52g, 30 mmol) in 50 mL H_2O was added to a solution of 1-methyl-*D*-tryptophan (Indoximod, 2.18g, 10 mmol) in THF (50 mL). The solution mixture was stirred in an ice bath for 30 min. Di-*tert*-butyl decarbonate (2.62g, 12 mmol) was then added into the reaction mixture, which was stirred at room temperature for 24 h and monitored by TLC. After

completion of the reaction, the reaction mixture was adjusted to pH = 1 with 1 M HCl aqueous solution, and the product was extracted with EtOAc. The organic phase was then washed with saturated brine and dried with anhydrous Na_2SO_4. The solvent was removed using rotary evaporator under vacuum, and the residue was used for the next step without further purification. White solid with 93% yield was obtained. R_f = 0.26 (petroleum/EtOAc = 1/1). ^{1}H NMR (400 MHz, $CDCl_3$) δ 7.62 (d, *J* = 7.9 Hz, 1H), 7.31 (d, *J* = 8.2 Hz, 1H), 7.25 (t, *J* = 7.4 Hz, 1H), 7.14 (dd, *J* = 10.9, 3.9 Hz, 1H), 6.93 (s, 1H), 5.05 (d, *J* = 5.0 Hz, 1H), 4.79 – 4.52 (m, 1H), 3.76 (s, 3H), 3.48 – 3.19 (m, 2H), 1.46 (s, 9H). LC/MS (ESI): 319.1 $[M + H]^+$.

2-((2-hydroxyethyl)disulfanyl)ethyl *N*$^{\alpha}$-(*tert*-butoxycarbonyl)-1-methyl-*D*-tryptophanate (Boc-IND-SS-OH).

EDCI (1.84 g, 9.6 mmol) and 6 mL DIPEA was added to a solution of Boc-IND (2.56 g, 8 mmol) in anhydrous DCM. The reaction mixture was stirred at room temperature for 30 min. Then a solution of 2,2'-disulfanediylbis(ethan-1-ol) (4.88 g, 32 mmol) in 20 mL THF was added into the mixture solution followed by addition of DMAP (98 mg, 0.8 mmol). The reaction solution was further stirred at room temperature for 12 h and monitored by TLC. After completion of the reaction, the solution mixture was washed with 50 mM HCl aqueous solution and then with saturated brine. The organic layer was dried with anhydrous Na_2SO_4, the solvent was evaporated using rotary evaporator under vacuum, and the residue was purified by silica gel flash chromatography. White solid with 85% yield was attained. R_f = 0.32 (petroleum/EtOAc = 2/1). ^{1}H NMR (400 MHz, $CDCl_3$) δ 7.52 (d, *J* = 7.9 Hz, 1H), 7.27 (d, *J* = 8.2 Hz, 1H), 7.22 – 7.16 (m, 1H), 7.09 (t, *J* = 7.4 Hz, 1H), 6.88 (s, 1H), 5.04 (d, *J* = 7.7 Hz, 1H), 4.60 (d, *J* = 6.5 Hz, 1H), 4.29 (ddd, *J* = 17.7, 11.8, 6.2 Hz, 2H), 3.81 (d, *J* = 5.4 Hz, 2H),

3.74 (s, 3H), 3.25 (d, *J* = 5.2 Hz, 2H), 2.86 – 2.62 (m, 4H), 1.41 (s, 9H). LC/MS (ESI): 455.1 $[M + H]^+$.

(*R*)-13,13-dimethyl-9-((1-methyl-1*H*-indol-3-yl)methyl)-8,11-dioxo-7,12-dioxa-3,4-dithia-10-azatetradecyl hydrazinecarboxylate (Boc-IND-SS-NH-NH_2).

CDI (0.98 g, 6 mmol) was added to a solution of Boc-IND-SS-OH (2.27 g, 5 mmol) in anhydrous DCM (50 mL). The reaction mixture was stirred at room temperature for 30 min and monitored by TLC until the formation of imidazolide was completed. Then hydrazine hydrate (0.5 mL) was added into reaction mixture and the solution was stirred for 2 h. The reaction mixture was monitored by TLC. After completion of the reaction, the solution mixture was washed with H_2O and then with saturated brine. The organic layer was dried with anhydrous Na_2SO_4, the solvent was evaporated using rotary evaporator under vacuum, and the residue was purified by silica gel flash chromatography. White solid with 82% yield was acquired. R_f = 0.28 (petroleum/EtOAc = 1/1). ^{1}H NMR (400 MHz, $CDCl_3$) δ 7.53 (d, *J* = 7.9 Hz, 1H), 7.27 (d, *J* = 8.2 Hz, 1H), 7.20 (t, *J* = 7.5 Hz, 1H), 7.09 (t, *J* = 7.1 Hz, 1H), 6.87 (s, 1H), 6.29 (s, 1H), 5.17 (d, *J* = 7.5 Hz, 1H), 4.62 (d, *J* = 6.3 Hz, 1H), 4.29 (t, *J* = 5.9 Hz, 4H), 3.72 (d, *J* = 6.5 Hz, 5H), 3.25 (d, *J* = 5.0 Hz, 2H), 2.87 (t, *J* = 6.2 Hz, 2H), 2.82 – 2.68 (m, 2H), 1.41 (s, 9H). LC/MS (ESI): 513.1 $[M + H]^+$.

2-((2-((1-methyl-*D*-tryptophyl)oxy)ethyl)disulfanyl)ethyl hydrazinecarboxylate (IND-SS-NH-NH_2).

Anisole (10 mL) was added to a solution of Boc-IND-SS-NH-NH_2 (2.563 g, 4 mmol) in anhydrous DCM (50 mL) followed by 2 mL CF_3COOH addition. The reaction mixture was

stirred at room temperature for 2 h and monitored by TLC. After completion of the reaction, the solvent was evaporated using rotary evaporator under vacuum, the mixture residue was dissolved in DCM and washed with saturated $NaHCO_3$ aqueous solution and then with saturated brine. The organic layer was dried with anhydrous Na_2SO_4, and the residue was purified by silica gel flash chromatography. Pale yellow solid with 62% yield was obtained. R_f = 0.26 (CH_2Cl_2/CH_3OH = 10/1). ^{1}H NMR (400 MHz, $CDCl_3$) δ 7.59 (t, *J* = 9.7 Hz, 1H), 7.30 (d, *J* = 8.1 Hz, 1H), 7.25 – 7.20 (m, 1H), 7.11 (t, *J* = 7.0 Hz, 1H), 6.95 (s, 1H), 6.23 (s, 1H), 4.36 (dd, *J* = 12.7, 6.3 Hz, 5H), 4.01 – 3.78 (m, 2H), 3.76 (s, 3H), 3.27 (dd, *J* = 14.3, 4.9 Hz, 1H), 3.05 (dd, *J* = 14.3, 7.6 Hz, 1H), 2.94 – 2.89 (m, 2H), 2.88 – 2.81 (m, 4H). HRMS (ESI) m/z $[M + H]^+$ for $C_{17}H_{25}N_4O_4S_2$ calculated 413.1312, found 413.1307.

2-((2-((1-methyl-*D*-tryptophyl)oxy)ethyl)disulfanyl)ethyl (*Z*)-2-(1-((2*S*,4*S*)-4-(((2*R*,4*S*,5*S*,6*S*)-4-amino-5-hydroxy-6-methyltetrahydro-2*H*-pyran-2-yl)oxy)-2,5,12-trihydroxy-7-methoxy-6,11-dioxo-1,2,3,4,6,11-hexahydrotetracen-2-yl)-2-hydroxyethylidene)hydrazine-1-carboxylate (DOX-IND).

10 μL CF_3COOH was added to a solution of IND-SS-NH-NH_2 (515 mg, 1.25 mmol) and Doxorubicin hydrochloride (696 mg, 1.20 mmol) in 10 mL absolute anhydrous CH_3OH. The solution mixture was stirred at room temperature for 36 h and monitored by TLC. After completion of the reaction, the suspension solution was placed under an ultrasonic bath for 10 min, the precipitation was filtered through a suction filtration. The solid was further mixed in 20 mL anhydrous acetonitrile and placed under an ultrasonic bath for 10 min, filtered, the product was obtained by repeating this procedure two times. Brick red solid with 47% yield was obtained. R_f = 0.37 ($CHCl_3$/EtOH/H_2O = 300/200/36). ^{1}H NMR (400 MHz, DMSO-d_6) δ

7.93 – 7.86 (m, 2H), 7.69 – 7.58 (m, 2H), 7.43 (d, *J* = 7.5 Hz, 1H), 7.28 (d, *J* = 7.9 Hz, 1H), 7.04 (t, *J* = 7.3 Hz, 1H), 6.98 – 6.88 (m, 1H), 5.45 – 5.33 (m, 2H), 5.27 (s, 1H), 5.13 (s, 1H), 5.05 (s, 1H), 4.99 – 4.89 (m, 1H), 4.83 (t, *J* = 5.6 Hz, 1H), 4.53 (d, *J* = 5.7 Hz, 1H), 4.47 – 4.32 (m, 2H), 4.31 – 4.20 (m, 2H), 4.13 (dd, *J* = 14.0, 10.0 Hz, 2H), 3.95 (d, *J* = 5.4 Hz, 3H), 3.66 (s, 3H), 3.50 (s, 1H), 3.44 – 3.36 (m, 1H), 3.14 (d, *J* = 17.2 Hz, 2H), 3.01 – 2.85 (m, 4H), 2.84 – 2.71 (m, 2H), 2.63 (s, 1H), 2.29 (s, 1H), 2.12 (s, 1H), 1.87 – 1.81 (m, 1H), 1.65 (dd, *J* = 9.4, 5.8 Hz, 1H), 1.13 (t, *J* = 6.0 Hz, 3H), 1.02 (t, *J* = 7.0 Hz, 1H). ^{13}C NMR (101 MHz, DMSO-d_6) δ 173.35, 170.94, 158.49, 156.19, 137.05, 136.98, 129.60, 128.97, 128.08, 127.99, 121.57, 119.34, 118.97, 118.86, 110.04, 109.93, 108.34, 107.66, 99.70, 66.59, 66.45, 64.39, 63.20, 62.99, 62.81, 62.36, 60.00, 59.89, 56.99, 56.47, 55.42, 54.68, 52.94, 52.55, 47.03, 45.74, 41.58, 41.53, 37.58, 37.31, 36.56, 32.82, 32.78, 28.69, 23.08, 19.01, 17.24, 9.02, 7.73. HRMS (ESI) m/z $[M + H]^+$ for $C_{44}H_{51}N_5O_{14}S_2$ calculated 938.2947, found 938.2935; HPLC retention time: 9.667 min.

Lactone stability analysis

1 mM DMSO stock solutions of CPT and SM-CPT conjugates (n = 3) were diluted to 50 μM by PBS (pH = 7.4) at 37 °C, respectively.[4, 5] At predetermined time points, an aliquot of the sample solutions was analyzed by HPLC/LC-MS (LCMS-2020, SHIMADZU) with the established analytic method presented in Supplemental Fig. 8. The closed lactone and open carboxylate forms, and CPT intermediate were determined by LC-MS, retention times, and area under the curve based on CPT and SM-CPT conjugates standards. The respective concentrations were calculated by fitting to the standard curve of CPT, CPT-intermediate or SM-CPT conjugates.

Cryo-EM

Liposomal suspensions (2 mg CPT/mL for Camptothesomes; 2.5 mg DOX-IND/mL for co-delivery Camptothesome-4, ~7% DOX-IND DLC) were prepared for imaging by applying 3 microliters to the surface of a C-Flat 1.2/1.3 engineered TEM grid (Protochips, Morrisville NC.) immediately followed by either a 3 or 6 second blot at 100% RH in a FEI Vitrobot (Hillsboro, OR.) prior to rapid emersion into liquid nitrogen cooled liquid ethane. Grids were transferred into a Phillips TF20 (Eindhoven NL.) operating at 120 KeV with a Gatan CT3500 side entry cryoholder (Pleasantville, CA.) maintained at -180 °C. Images were recorded on a TVIPS XF416 CMOS camera at the indicated and measurements were performed within the EMMenu software package provided by TVIPS (Gauting, DE) for the operation of the XF416 camera.

Drug release kinetics of Camptothesome-4

The *in vitro* drug release kinetics study of Camptothesome-4 was carried out by dialysis using PBS (pH = 7.4, or GSH = 10 mM) containing 0.5% (w/v) Tween 80 as the release medium. Two mL of Camptothesome-4 (1 mg CPT/mL) were sealed in dialysis tubes (MWCO = 12 kDa, Spectrum Laboratories) which were then immersed in 50 mL release medium in a beaker covered with aluminum foil. The beakers were maintained at 37 °C with stirring at 100 rpm. 5 μL and 100 μL of solution were taken from the dialysis tubes and dialysate at various time points, respectively. The concentration of SM-CSS-CPT and CPT remaining in the dialysis tubes and dialysate were measured by HPLC with the detector set at 254 nm.

Preparation of CPT-loaded liposomes

An appropriate ratio of phospholipid (SM, HSPC, DSPC, DOPC, SPC or Lecithin), cholesterol and DSPE-PEG_{2K} (Avanti Polar Lipids) as listed in Supplementary Fig. 9d were dissolved in ethanol in a 100 mL round bottom flask, CPT (10 % weight of phospholipid) was added into the solution and the mixture was completely dissolved by sonication for 10-20 min. The solvent was evaporated under a rotatory evaporator (RV 10 digital, IKA®) to generate a thin film, which was further dried under ultra-high vacuum (MaximaDry, Fisherbrand) for 0.5 h. The film was hydrated with 5% dextrose aqueous solution at 50 °C for 30 min, and then sonicated for 12 min by using a pulse 3/2 s on/off at a power output of 60 W. To remove any unloaded CPT, the nanoparticles were purified by running through a PD-10 column. The size and zeta potential, and CPT content of the purified CPT-loaded liposomes were measured by the Zetasizer Nano (Nano-ZS, Malvern Panalytical) and HPLC, respectively. CPT drug loading capacity [DLC, equation (4)] was calculated as below:

$$\text{equation (4)} = \frac{\text{weight of CPT loaded in liposome}}{\text{weight of liposome} + \text{weight of CPT loaded in liposome}} \times 100\%$$

Cells and mice

CT26 and CT26-Luc were obtained from UACC and cultured in complete RPMI-1640 medium. MC38 was purchased from Kerafast and cultured in complete DMEM medium. B16-F10-Luc2 was obtained from ATCC and cultured in complete DMEM medium. All the cell lines were cultured in the corresponding medium containing 10% FBS, 100 U/mL penicillin, 100 μg/mL streptomycin, and 2 mM L-glutamine at 37 °C in a CO_2 incubator. BALB/c and

C57BL/6 mice (Charles Rivers, 6-8 weeks old, male and female) were used. Tumour size was measured by a digital caliper at indicated times and calculated according to the formula=0.5 × length × width^2. Mice were removed from the respective study when tumour was found to be > 2000 mm^3 or animals became moribund with severe weight loss, extreme weakness or inactivity. The animals were maintained under pathogen-free conditions and all animal experiments were approved by the University of Arizona Institutional Animal Care and Use Committee (IACUC).

MTD

Groups of 3 BALB/c mice were administered intravenously (IV) with free CPT (5, 7.5, 10, and 12.5 mg CPT/kg, formulated in 10% Tween 80/0.9% NaCl (9:1, v/v) with 20 min probe sonication)[6], Camptothesome-1 (50, 65, 80, 100, and 120 mg CPT/kg), Camptothesome-2 (15, 25, 35, 40, and 45 mg CPT/kg), Camptothesome-3 (15, 25, 30, 35, 40, 45, 60, and 80 mg CPT/kg), Camptothesome-4 (15, 25, 30, 35, 40, and 45 mg CPT/kg) and DOX-IND/Camptothesome-4 (5/15, 6.7/20, 8.3/25, and 10/30 mg DOX-IND/CPT mg/kg). Changes in body weight and survival of mice were followed every 1-2 days for two weeks. The MTD was defined as the dose that causes neither mouse death due to the toxicity nor greater than 15% of body weight loss or other remarkable changes in the general appearance within the entire period of the experiments. On day 14 post drug injection, blood was withdrawn by cardiac puncture and major organs (e.g., heart, liver, and kidneys) were collected. Blood was collected in lithium heparin tubes (BD Microtainer™) followed by centrifuging at 2,000 g for 10 minutes in a refrigerated centrifuge. The supernatant (serum) was sent to University Animal Care Pathology Services Core at UArizona for a series of serum chemistry analysis (Liasys 330).

The whole blood in dipotassium EDTA tube (BD Microtainer™) were used for leukocytes, erythrocytes, and thrombocytes analysis (Hemavet 950FS). Mice organs from MTD dose and vehicle control groups were placed in a 4% paraformaldehyde solution for 24 h and then sent to Tissue Acquisition and Cellular/Molecular Analysis Shared Resource (TACMASR) at UArizona Cancer Center (UACC) for histopathological analysis.

Immunohistochemistry (IHC)

The tumour blocks from respective therapeutic efficacy studies were collected from sacrificed mice, fixed in 4% paraformaldehyde overnight, processed and then embedded by paraffin. Tumour blocks were cut into sections of 4 μm thickness, which were mounted on positively charged glass slides by the UACC TACMASR Core facility for a series of IHC staining processes and procedures following established protocols. Briefly, the slides were loaded onto the Leica Bond RXm Autostainer with covertiles to prevent dehydration between staining steps. Slides were heated to 60 °C then deparaffinized. Slides were incubated in 10 mM tris-EDTA (pH = 9) or 1 mM sodium citrate (pH = 6) at 98 °C (85 °C for Calreticulin; 50 °C for Perforin) for epitope retrieval. After cooling down to ambient temperature, the slides were rinsed in TBS wash buffer and were subsequently treated with 3% H_2O_2 for 5 min to block endogenous peroxidase activity, and then incubated with individual primary antibodies for 15 to 50 minutes. Afterwards, the slides were rinsed with wash buffer and followed by incubation with HRP-conjugated anti-rabbit polymer; for Foxp3 and IL-10, rabbit anti-rat secondary antibody was used prior to incubation with HRP-conjugated anti-rabbit polymer at ambient temperature for 8 min. The slides were incubated with DAB (3,3′-Diaminobenzidine) for 10 minutes for visualization after being rinsed with wash buffer. Whereafter, the slides were

washed in distilled water, counterstained with Hematoxylin at room temperature for 5 minutes. The reagents are part of the Bond Polymer Refine Detection Kit (DS9800, Leica). Slides were unloaded from the Autostainer, dehydrated in increasing concentrations of ethanol, three changes of xylene, mounted with media and a cover-slipped. After staining, the slide sections were dried and observed under microscope [NIS-Elements F software (v. 4.00.00), Nikon, Eclipse 50i, Japan] equipped with a digital camera. The slides were read by an experienced veterinary pathologist and the semi-quantification of the IHC staining intensity of each immune biomarker was obtained by dividing the mean DAB staining intensity value by the total number of nuclei measured by the ImageJ Fiji software (v. 1.2) following the established protocol.[7]. Afterwards, the respective IHC staining semi-quantitative data was normalized to vehicle control samples.

Antibodies utilized for IHC staining

Anti-interferon gamma (ab9657, 1/200), anti-PD-1 (ab137132, 1/500), anti-IDO (ab106134, 1/300), anti-HMGB1 (ab18256, 1/400), anti-TLR4 (ab13867, 1/100), anti-IL-12 (ab131039, 1/500), anti-IL-10 (ab189392, 1/100), anti-LRP1 (ab92544, 1/750), anti-CD8α (ab209775, 1/100), anti-perforin (ab16074, 1/600), anti-granzyme B (ab4059, 1/100), and anti-calreticulin (ab2907, 1/400) were obtained from Abcam; Anti-PD-L1 (#13684T, 1/75) and anti-cleaved caspase-3 (#9664S, 1/300) were purchased from Cell Signaling; Anti-Foxp3 (#13-5773-82, 1/100) was from Invitrogen. All antibodies were diluted in Bond Primary Antibody Diluent (AR9352, Leica).

Foxp3 and IL-10 used a rabbit anti-mouse secondary antibody prior to incubating with the HRP-conjugated anti-rabbit polymer. TLR4, LRP1, HMGB1, Granzyme B, CD8, CC3, IL-12, PD-L1, and Calreticulin did not require a secondary antibody as they were rabbit antibodies and the HRP-conjugated polymer on the staining kit is against rabbit.

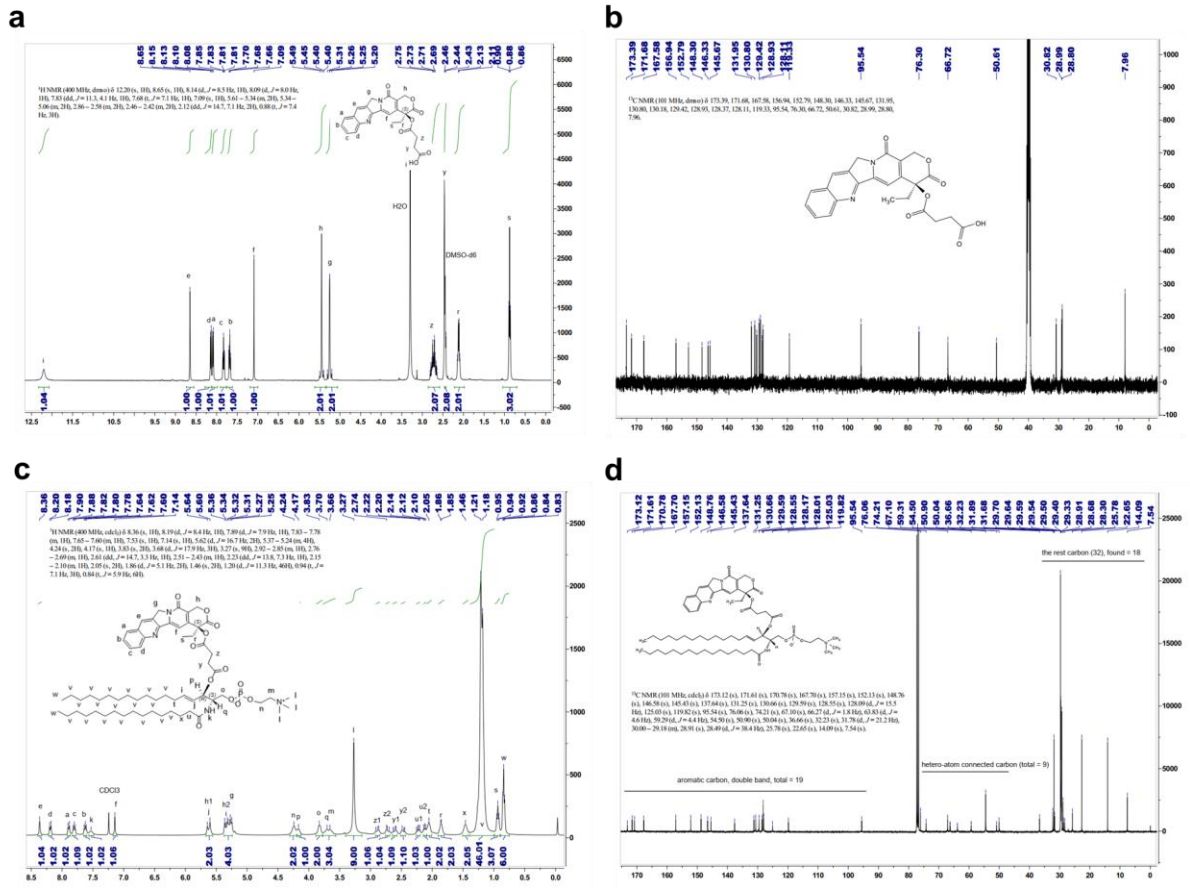

Supplementary Figure 1. ^{1}H NMR and ^{13}C NMR spectra for CPT-COOH (**a, b**) and SM-Ester-CPT (**c, d**).

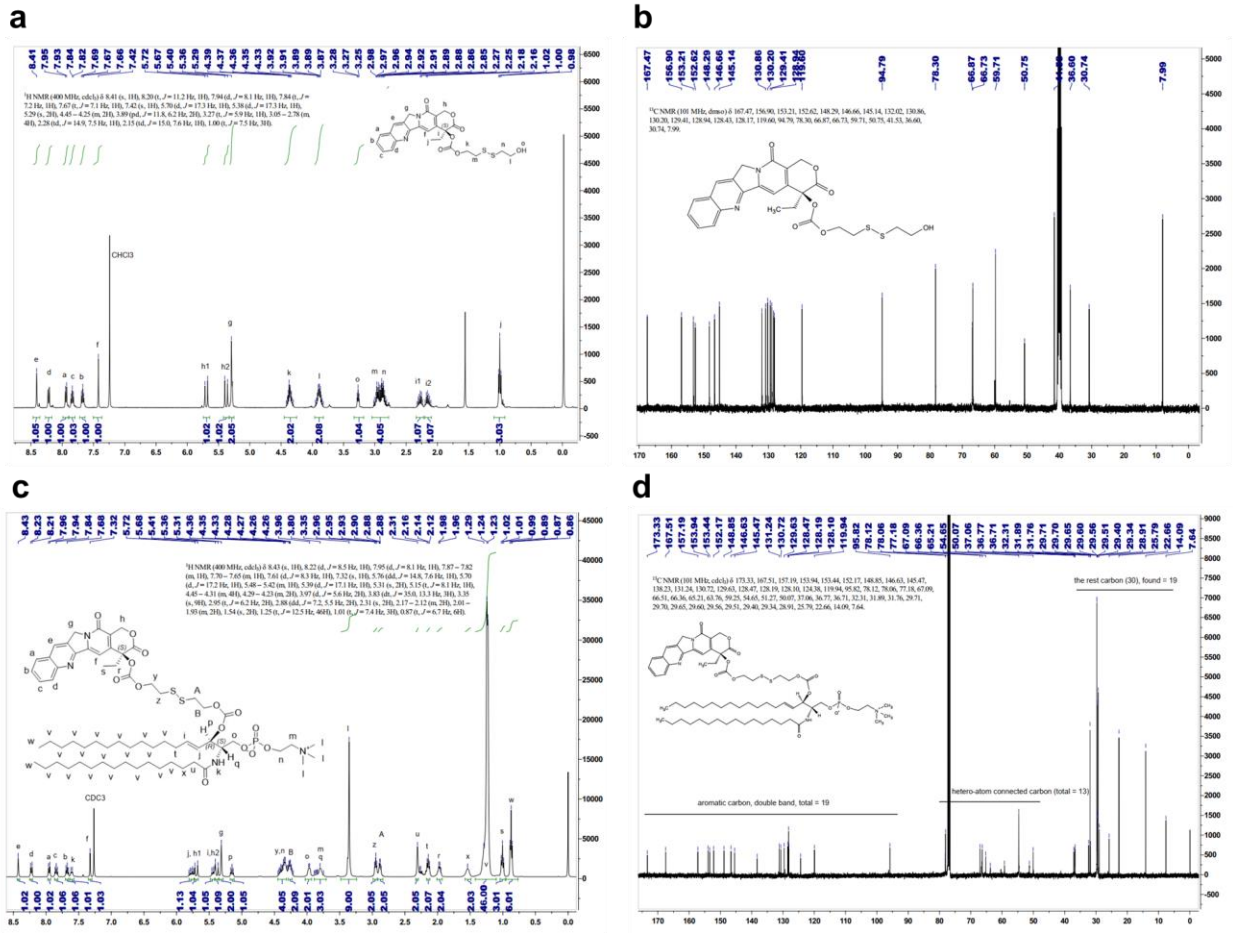

Supplementary Figure 2. ^{1}H NMR and ^{13}C NMR spectra for CPT-SS-OH (**a, b**) and SM-SS-CPT (**c, d**).

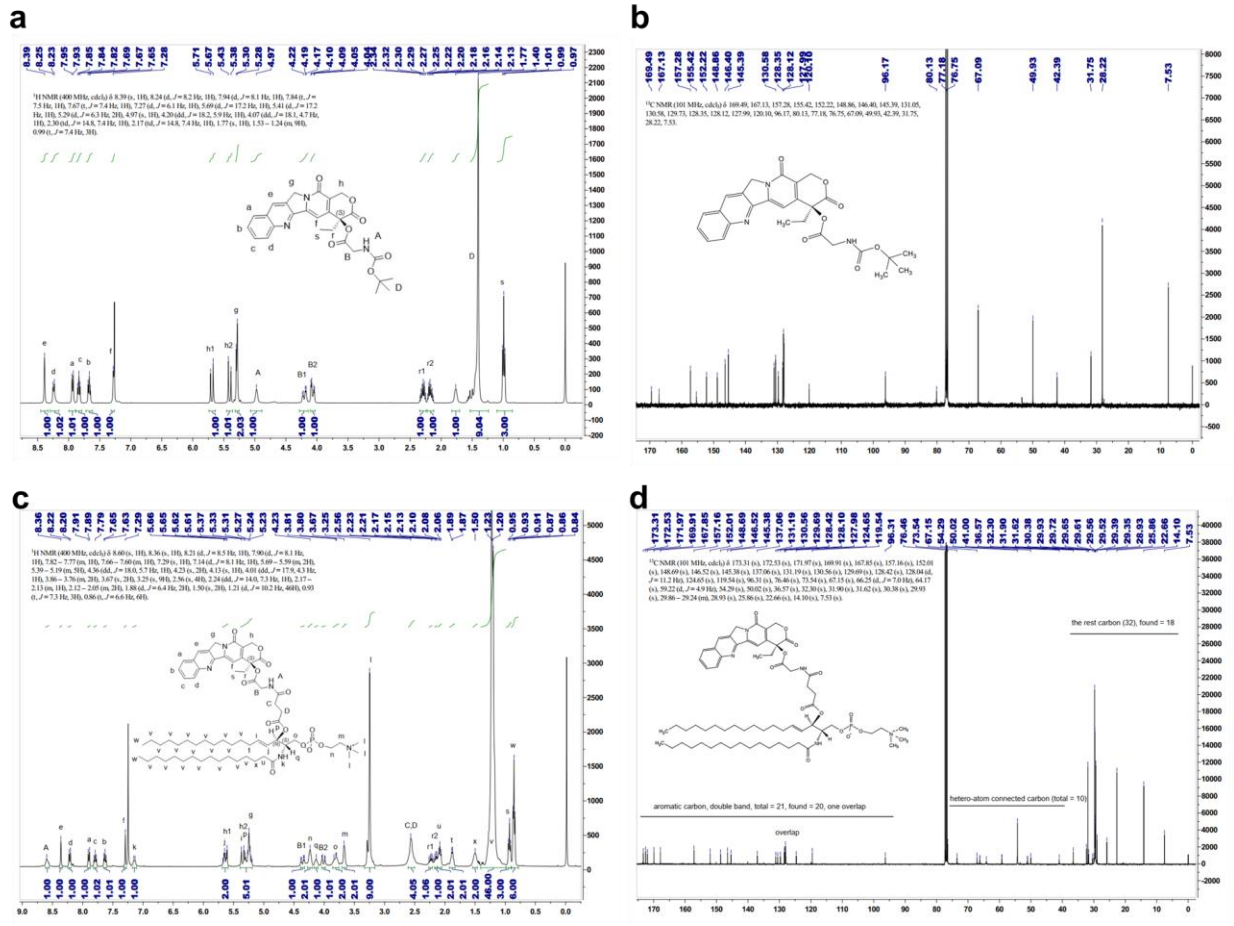

Supplementary Figure 3. ^{1}H NMR and ^{13}C NMR spectra for CPT-Glycine-Boc (**a, b**), CPT-Glycine (**c, d**), and SM-Glycine-CPT (**e, f**).

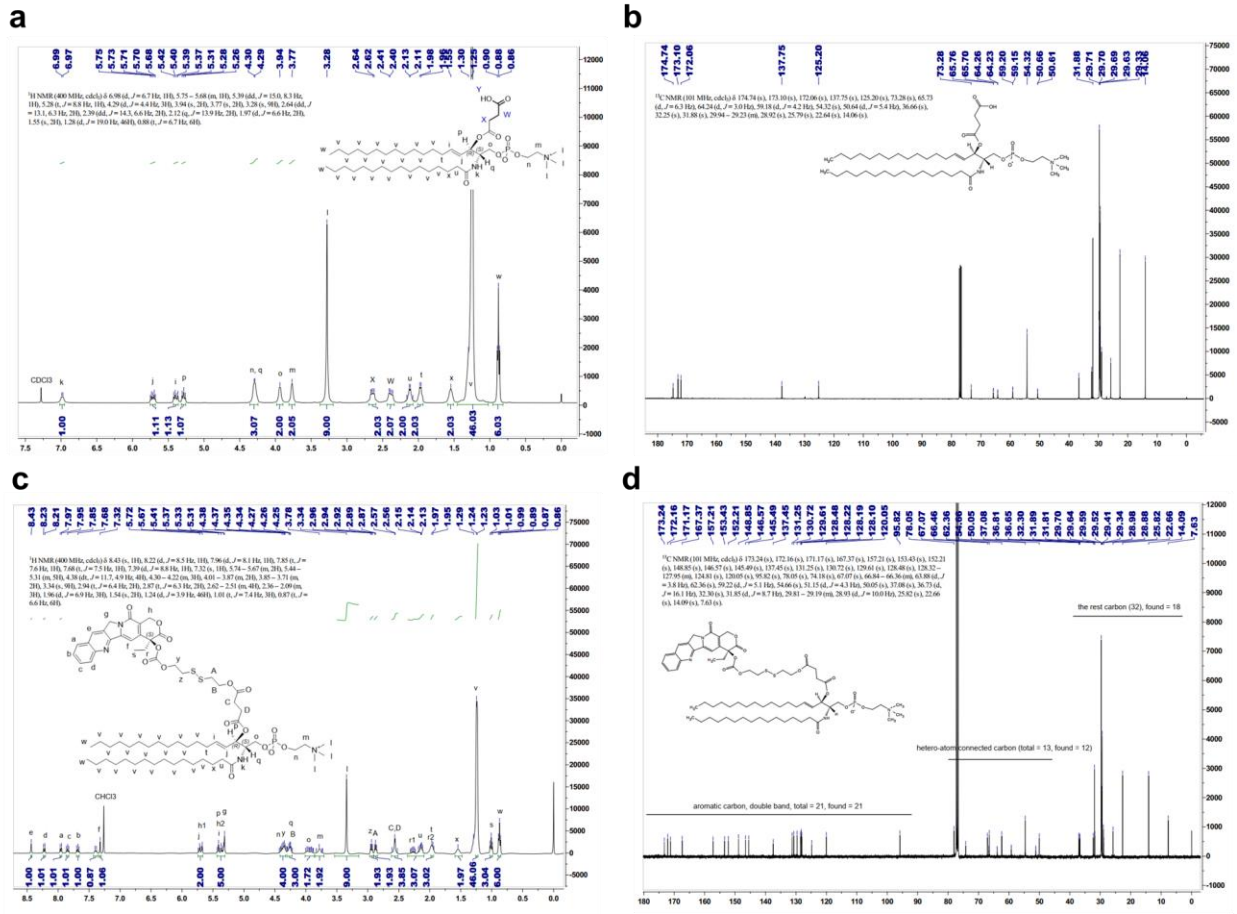

Supplementary Figure 4. ^{1}H-NMR and ^{13}C-NMR spectra for SM-COOH (**a, b**) and SM-CSS-CPT (**c, d**).

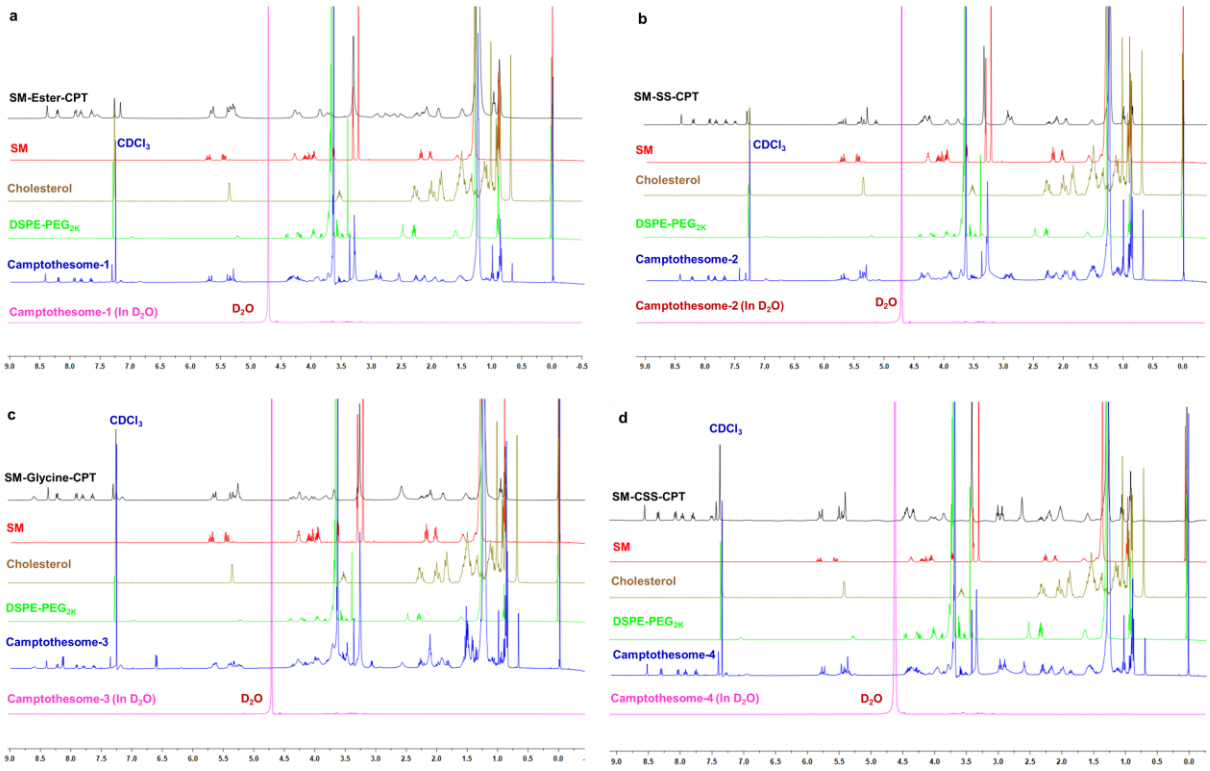

Supplementary Figure 5. ^{1}H NMR spectra of Camptothesome-1 (**a**), Camptothesome-2 (**b**), Camptothesome-3 (**c**), Camptothesome-4 (**d**), in D_2O, and their respective SM-CPT conjugate, SM, Cholesterol, and DSPE-PEG_{2K} in $CDCl_3$.

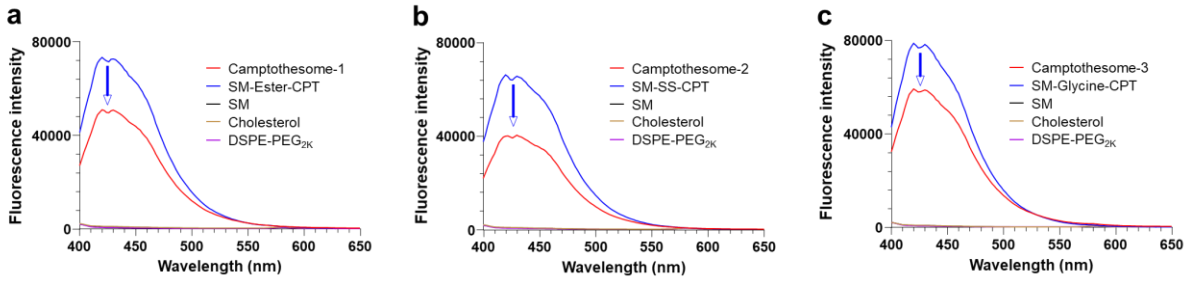

Supplementary Figure 6. Fluorescence quenching of SM-Ester-CPT (**a**), SM-SS-CPT (**b**), and SM-Glycine-CPT (**c**) upon self-assembling into Camptothesome. Experiments were independently repeated for three times.

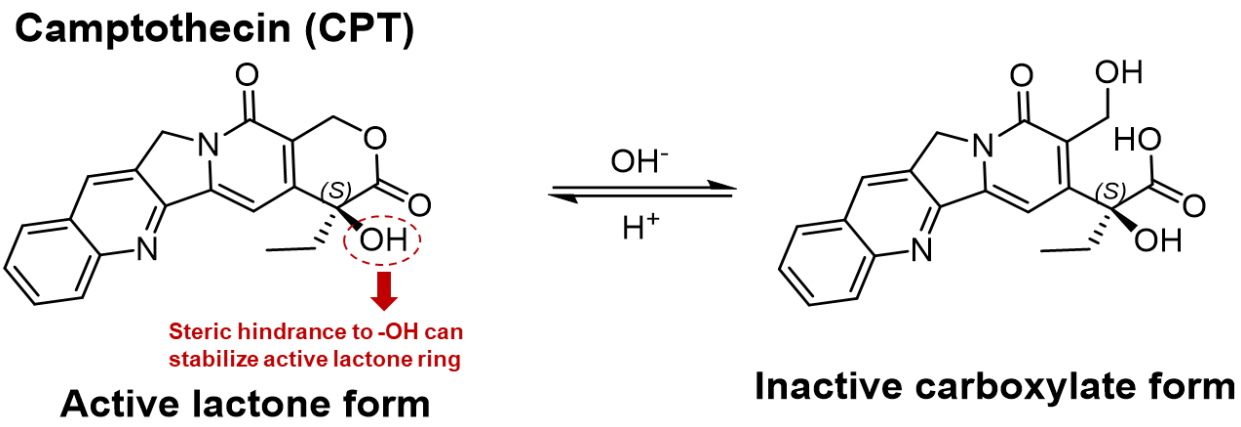

Supplementary Figure 7. CPT chemical structure and pH-dependent equilibrium between the active lactone and inactive carboxylate form**.** Introducing steric hindrance to the hydroxyl group of CPT has been shown to enhance the lactone ring stability[4, 5].

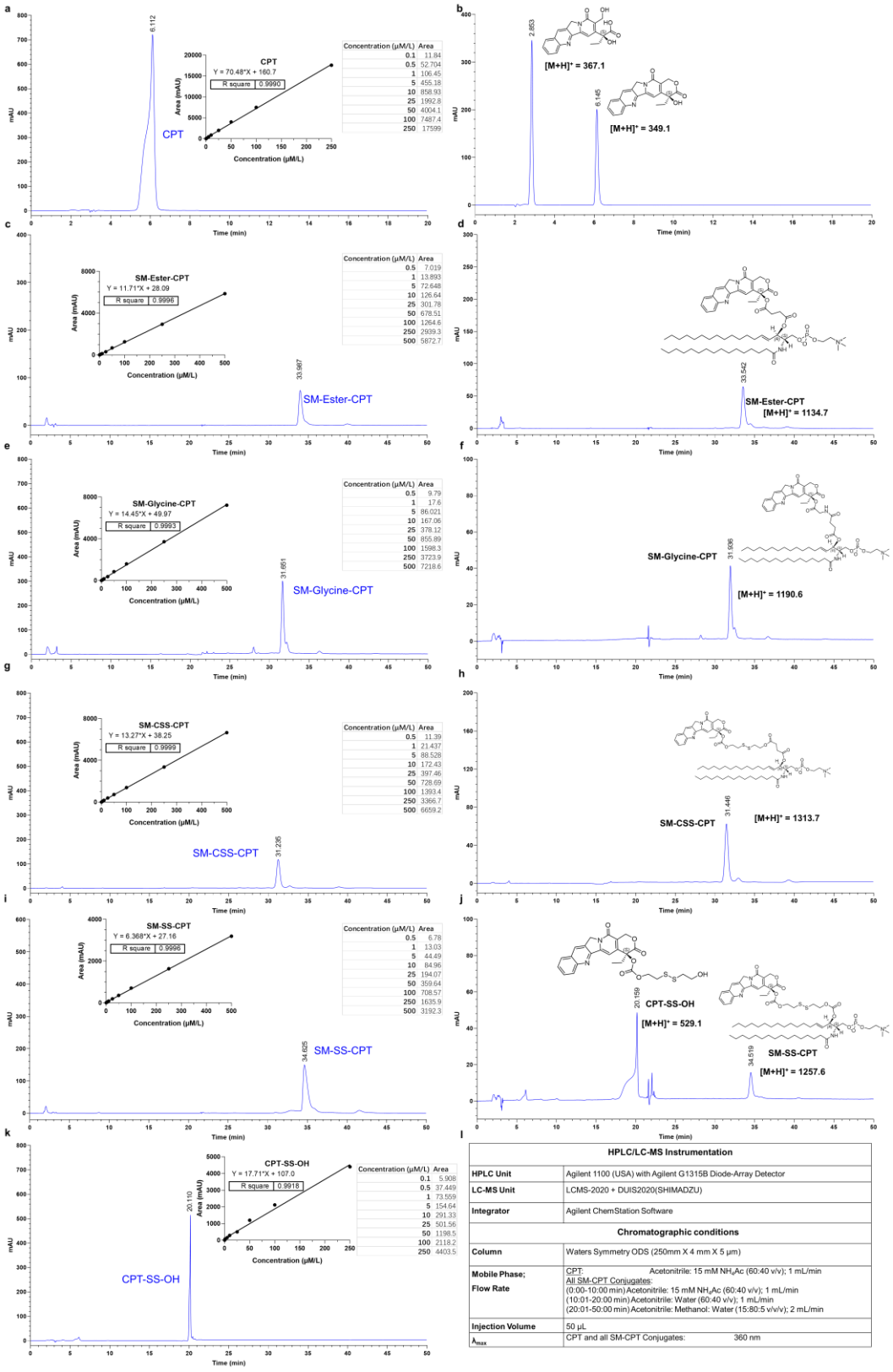

Supplementary Figure 8. Analytic Reverse-phase High Performance Liquid Chromatography (HPLC) and Liquid Chromatography–Mass Spectrometry (LC-MS) method development for lactone stability study in **Fig. 1l**. **a-k**, respective representative HPLC chromatogram and

standard curve for CPT (**a**), SM-Ester-CPT (**c**), SM-Glycine-CPT (**e**), SM-CSS-CPT (**g**), SM-SS-CPT (**i**), and CPT-SS-OH (**k**). LC-MS was used to verify the identity of target compounds. Respective representative HPLC chromatogram and ESI-MS for free CPT (**b**, lactone and carboxylate forms), SM-Ester-CPT (**d**), SM-Glycine-CPT (**f**), SM-CSS-CPT (**g**), SM-SS-CPT and CPT-SS-OH (**j**), (**l**) A table summarizing the detailed information for HPLC/LC-MS instrumentation and chromatographic conditions.

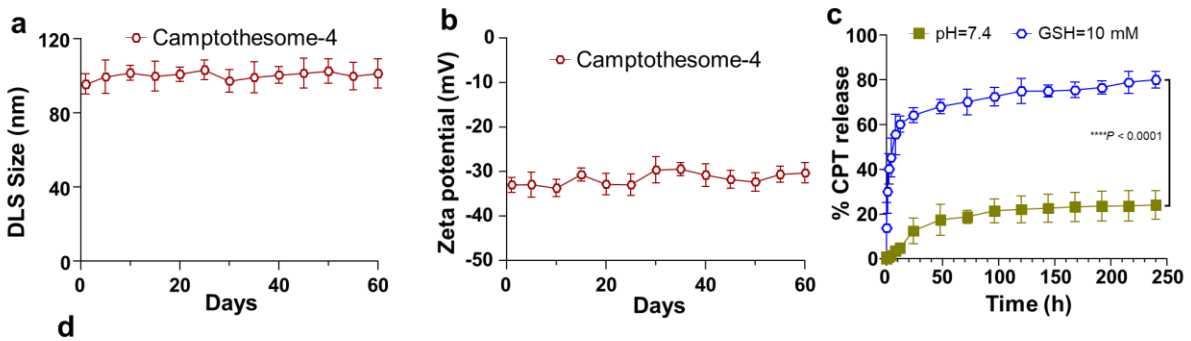

d

CPT-loaded liposomes	Phospholipid (molar %)	Cholesterol (molar %)	DSPE-PEG$_{2K}$ (molar %)	CPT DLC (weight %)	DLS size (nm)	Zeta potential (mV)	Polydispersity index
CPT/Lipo-SM	84.41 (SM)	11.03	4.56	0.14 ± 0.08	199.46 ± 21.89	-16.33 ± 2.49	0.195 ± 0.072
CPT/Lipo-HSPC	83.44 (HSPC)	11.72	4.84	0.13 ± 0.05	113.30 ± 12.56	-13.29 ± 4.57	0.173 ± 0.089
CPT/Lipo-DSPC	82.93 (DSPC)	12.08	4.99	0.08 ± 0.03	141.91 ± 9.24	-9.85 ± 2.76	0.208 ± 0.051
CPT/Lipo-DOPC	82.99 (DOPC)	12.03	4.98	0.11 ± 0.10	164.91 ± 14.98	-18.02 ± 3.18	0.217 ± 0.037
CPT/Lipo-SPC	83.2 (SPC)	11.89	4.91	0.07 ± 0.02	178.65 ± 19.66	-20.08 ± 5.64	0.188 ± 0.044
CPT/Lipo-Lecithin	84.1 (Lecithin)	11.25	4.65	0.08 ± 0.04	187.77 ± 17.87	-22.12 ± 4.15	0.198 ± 0.076

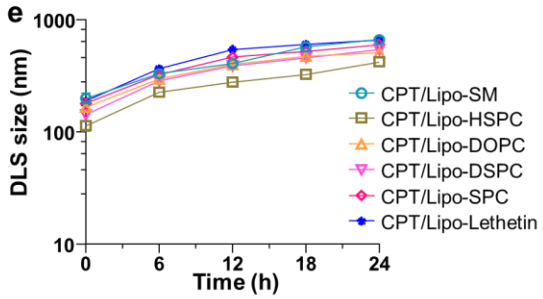

Supplementary Figure 9. a,b, The DLS size (**a**) and zeta potential (**b**) monitoring for Camptothesome-4 over a 60-day period after preparation in 5% dextrose at 4 °C. **c**, The CPT release kinetics of Camptothesome-4 under different conditions at 37 °C. **d**, Physicochemical characterizations of six different CPT-loaded (physically) liposomes. **e**, Size change over time in 5% dextrose at 4 °C. Data are represented as mean ± SD (n = 3 independent experiments). ****P < 0.0001 (two-tailed, unpaired Student's t-test).

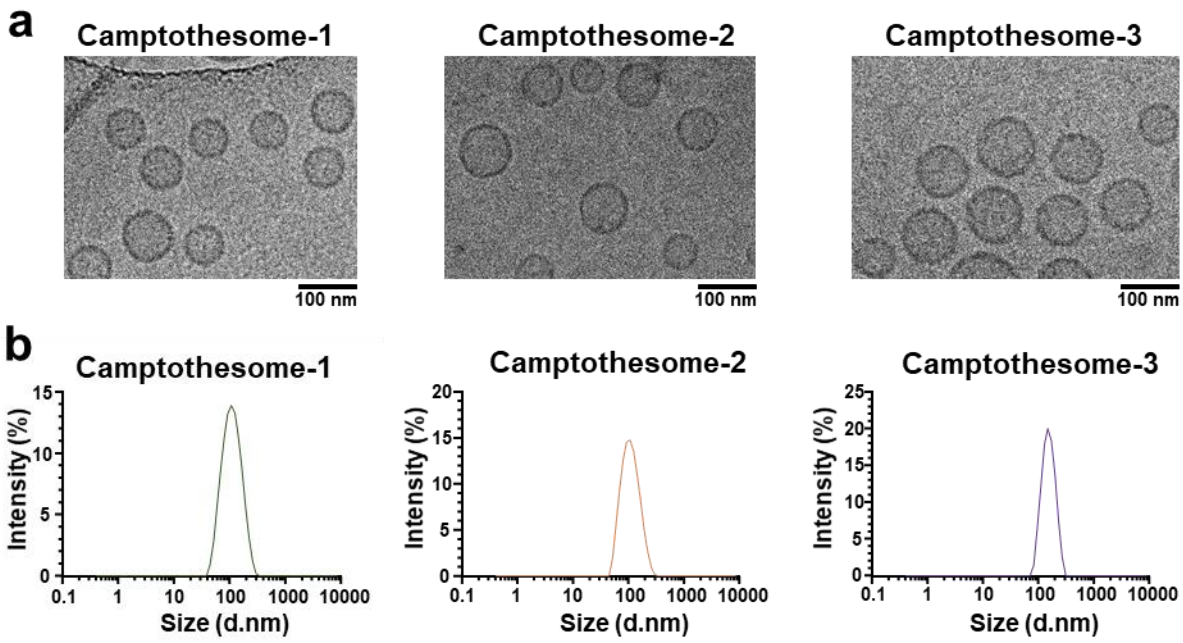

Supplementary Figure 10. The representative CryoEM images (**a**) and DLS size distribution by intensity for Camptothesome-1, Camptothesome-2, and Camptothesome-3 (**b**, experiments were independently repeated for three times)

Formulation	Dose (mg/kg)	Animal death	Weight loss (%)
Free CPT	5	0/3	1.82 ± 2.96
	7.5	1/3	N/A
	10	1/3	N/A
	12.5	0/3	25.35 ± 5.37
Camptothesome-1	50	0/3	-2.62 ± 2.48
	65	0/3	4.24 ± 7.13
	80	0/3	-3.56 ± 1.79
	100	0/3	0.39 ± 1.39
	120	0/3	0.46 ± 0.96
Camptothesome-2	15	0/3	0.31 ± 5.11
	25	0/3	0.51 ± 2.00
	30	0/3	11.3 ± 0.57
	35	2/3	N/A
	40	2/3	N/A
	45	3/3	N/A
Camptothesome-3	15	0/3	3.87 ± 2.05
	25	0/3	0.57 ± 0.43
	35	0/3	1.78 ± 0.56
	40	0/3	1.55 ± 1.12
	45	0/3	2.98 ± 0.83
	60	0/3	-0.03 ± 0.13
	80	0/3	-2.99 ± 1.15
Camptothesome-4	15	0/3	2.23 ± 0.63
	25	0/3	3.33 ± 1.78
	30	0/3	0.89 ± 0.58
	35	1/3	N/A
	40	1/3	N/A
	45	2/3	N/A

Supplementary Figure 11. MTD Investigation as shown in Fig. 2 for free CPT, Camptothesome-1, Camptothesome-2, Camptothesome-3, Camptothesome-4. Weight loss data are represented as mean ± SD (n = 3 mice).

a **Physicochemical characterizations of Cy5.5-labeled/Camptothesome-4**

Formulation	DSPE-Cy5.5 (w/w%)	DLS size by intensity (d.nm)	Zeta potential (mV)	Polydispersity index
Cy5.5/Camptothesome-4	0.1%	169.1 ± 10.51	-28.9 ± 2.50	0.204 ± 0.047
	0.2%	95.5 ± 4.12	-31.0 ± 3.28	0.167 ± 0.022
	0.3%	118.3 ± 5.76	-28.7 ± 1.00	0.210 ± 0.034

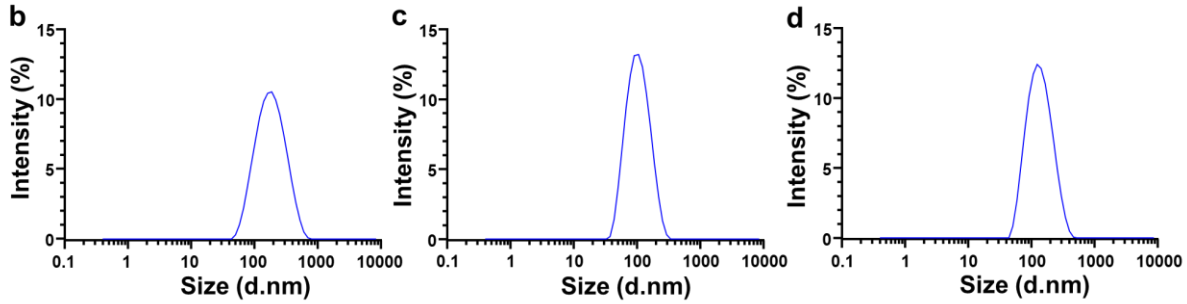

Supplementary Figure 12. Development and physicochemical characterizations of Cy5.5-labeled-Camptothesome-4. **a,** A table shows the physicochemical characterizations of Cy5.5/Camptothesome-4 with regards to size, zeta potential and polydispersity (mean ± SD) using different molar ratios of DSPE-Cy5.5. **b-c,** The representative DLS size distribution by intensity for 0.1 weight % (**b**), 0.2 weight % (**c**), or 0.3 weight % (**d**) of DSPE-Cy5.5 in Cy5.5/Camptothesome-4. Experiments were independently repeated for three times.

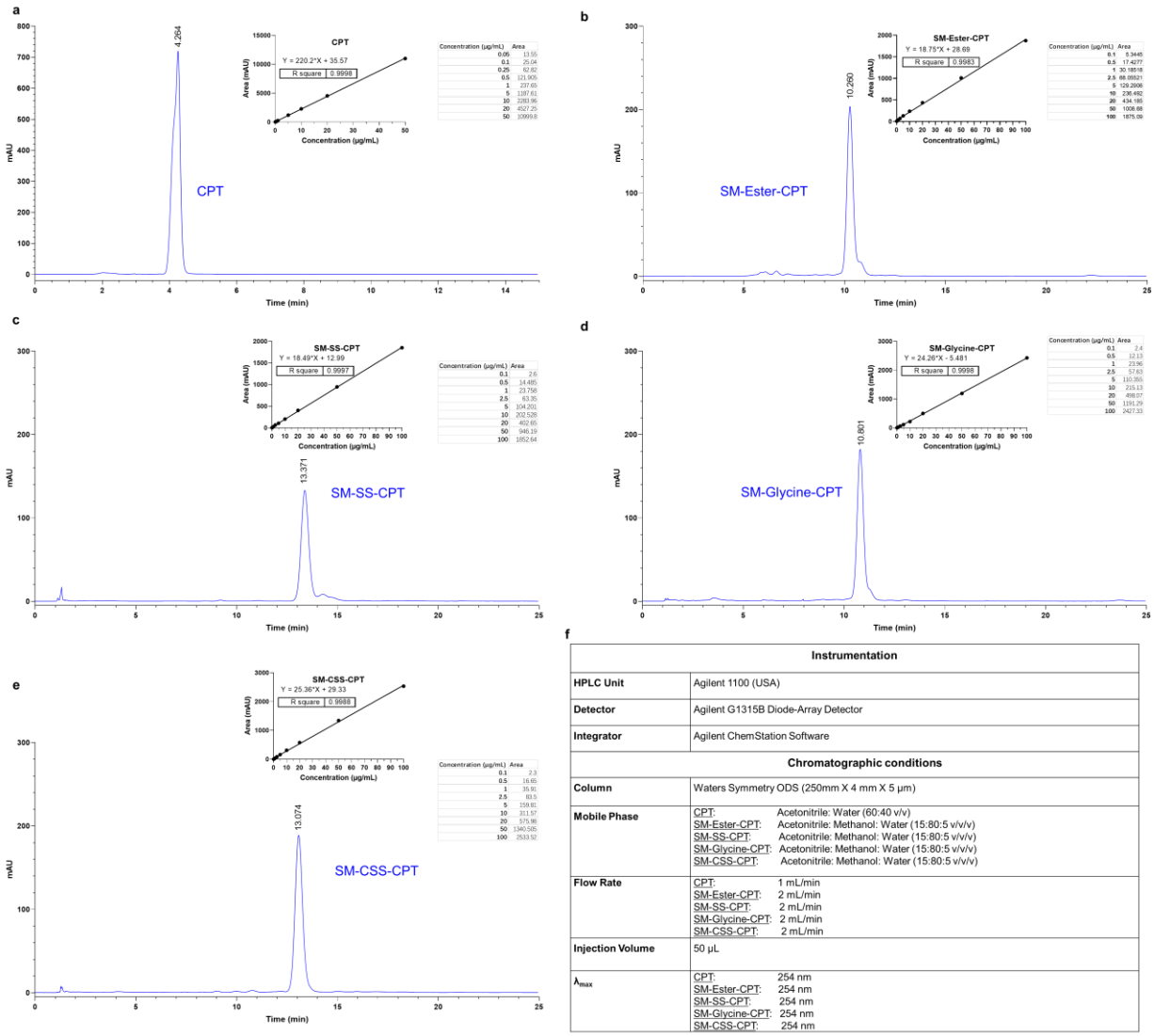

f

Instrumentation	
HPLC Unit	Agilent 1100 (USA)
Detector	Agilent G1315B Diode-Array Detector
Integrator	Agilent ChemStation Software
Chromatographic conditions	
Column	Waters Symmetry ODS (250mm X 4 mm X 5 μm)
Mobile Phase	CPT: Acetonitrile: Water (60:40 v/v) SM-Ester-CPT: Acetonitrile: Methanol: Water (15:80:5 v/v/v) SM-SS-CPT: Acetonitrile: Methanol: Water (15:80:5 v/v/v) SM-Glycine-CPT: Acetonitrile: Methanol: Water (15:80:5 v/v/v) SM-CSS-CPT: Acetonitrile: Methanol: Water (15:80:5 v/v/v)
Flow Rate	CPT: 1 mL/min SM-Ester-CPT: 2 mL/min SM-SS-CPT: 2 mL/min SM-Glycine-CPT: 2 mL/min SM-CSS-CPT: 2 mL/min
Injection Volume	50 μL
λ_{max}	CPT: 254 nm SM-Ester-CPT: 254 nm SM-SS-CPT: 254 nm SM-Glycine-CPT: 254 nm SM-CSS-CPT: 254 nm

Supplementary Figure 13. Analytic Reverse-phase High Performance Liquid Chromatography (HPLC) method development for free CPT and SM-derived CPTs in pharmacokinetics and biodistribution studies (**Fig. 3a-c**). **a-e,** respective representative HPLC chromatogram and standard curve for CPT (**a**), SM-Ester-CPT (**b**), SM-SS-CPT (**c**), SM-Glycine-CPT (**d**), SM-CSS-CPT (**e**). (**f**) Detailed information for HPLC instrumentation and chromatographic conditions.

	Free CPT	Camptothesome-2	Camptothesome-3	Camptothesome-4
$T_{1/2}$ (h)	0.07 ± 0.01	2.73 ± 0.58	0.13 ± 0.10	3.64 ± 0.09
V ((µg)/(µg/ml))	26.44 ± 0.27	1.13 ± 0.04	5.30 ± 2.00	1.15 ± 0.03
CL(µg)/(µg/ml)/h)	36.06 ± 5.00	0.29 ± 0.05	1.18 ± 0.47	0.22 ± 0.01
AUC_{0-t} (µg/ml*h)	10.95 ± 1.55	1378.24 ± 243.30	329.04 ± 93.03	1810.72 ± 43.90
AUC_{0-inf} (µg/ml*h)	11.25 ± 1.52	1382.89 ± 247.50	377.09 ± 153.6	1829.81 ± 45.62
AUMC (µg/ml*h^2)	65.42 ± 6.99	5586.61 ± 2057.51	4277.30 ± 2086.16	9618.66 ± 438.55
MRT (h)	5.85 ± 0.41	3.94 ± 0.84	9.95 ± 5.76	5.25 ± 0.14
V_{ss} (µg/(µg/ml))	211.68 ± 38.45	1.13 ± 0.05	10.41 ± 3.03	1.15 ± 0.03

Supplementary Figure 14. A table depicting a series of pharmacokinetic parameters for Free CPT, Camptothesome-2, Camptothesome-3, and Camptothesome-4 from the pharmacokinetics study shown in **Fig. 3a**. Data are represented as mean ± SD (n = 3 mice).

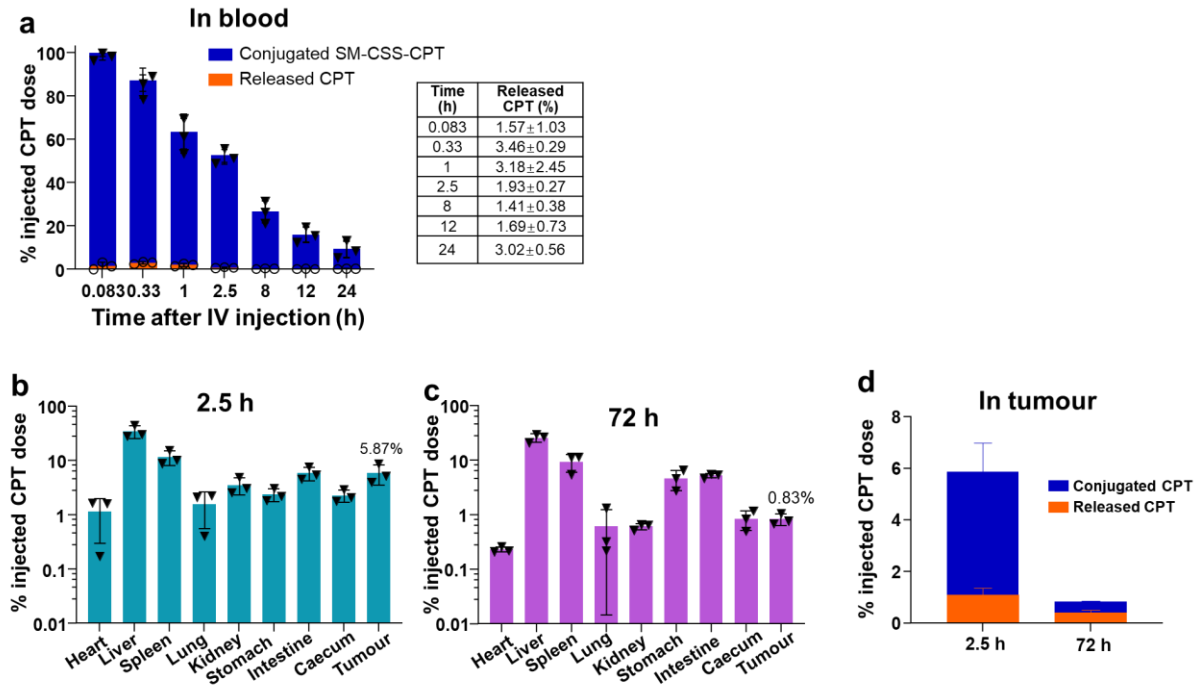

Supplementary Figure 15. a, CPT release in blood from Camptothesosome-4 in **Fig. 3a**. **b-d,** Tissue distribution for Camptothesome-4. An independent biodistribution study was performed in subcutaneous (SC) CT26 tumour-bearing BALB/c mice (tumours: ~300 mm^3) at 2.5 h (**b**) and 72 h (**c**) post IV administration of Camptothesome-4 (20 mg CPT/kg). **d**, intratumoural release of CPT at 2.5 h and 7.2 h from mice (**b**,**c**). Data are represented as mean ± SD (n = 3 mice).

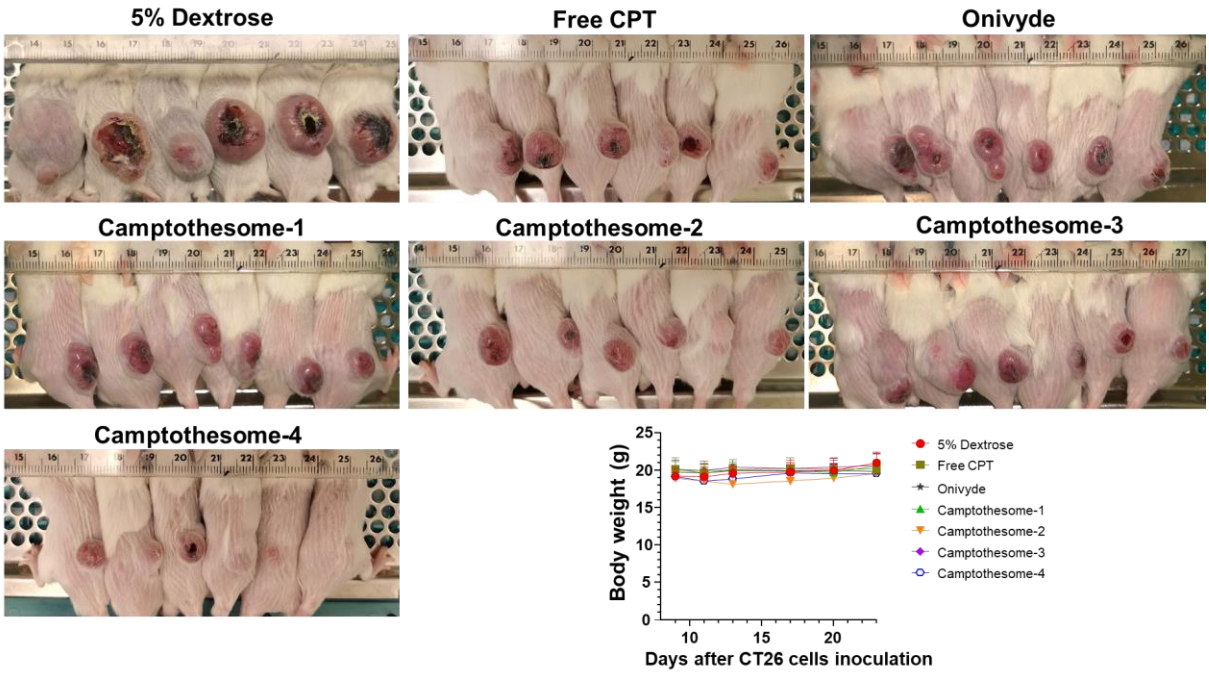

Supplementary Figure 16. Tumour-bearing mice images taken on day 24 and the mice body weight from the antitumour efficacy study shown in **Fig. 4a, b.** Body weight data are represented as mean ± SD (n = 6 mice).

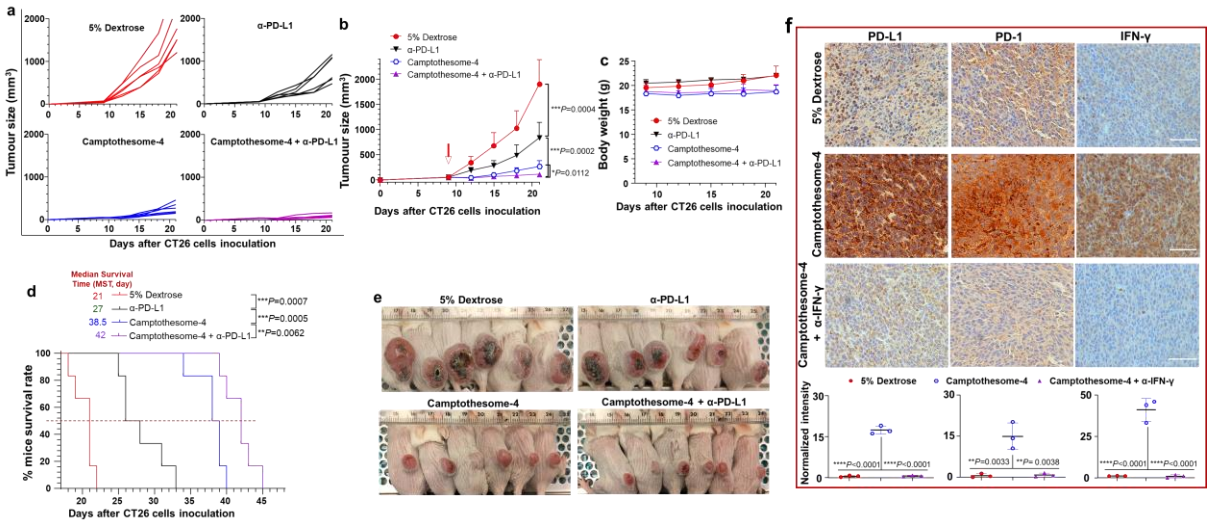

Supplementary Figure 17. Therapeutic efficacy of combing α-PD-L1 and Camptothesome-4 in SC CT26 tumour murine model. Mice were SC inoculated with 1×10^5 CT26 cells on day 0. On day 9, mice (n=6, ~50 mm^3) were IV administered once by 5% dextrose (vehicle control), or Camptothesome-4 (20 mg CPT/kg). α-PD-L1 was IP injected (100 μg/mouse) from day 9 every 3 days for 3 times. **a**, Individual tumour growth curves. **b**, Average tumour growth curves. **c**, Mice body weight monitoring. **d**, Kaplan–Meier survival curves. **e**, Tumour-bearing mice images taken on day 22. **f**, Tumour IHC staining (PD-L1, PD-1, and IFN-γ) at day 7 post IV administering Camptothesome-4 (20 mg CPT/kg) once to CT26 tumour-bearing mice (n=3 mice; tumours: ~200 mm^3), Scale bar=100 μm. Data in (**b, c, f**) are expressed as mean ± SD. **P* < 0.05, ***P* < 0.01, ****P* < 0.001, *****P* < 0.0001 (Statistical significance was determined by one-way ANOVA followed by Tukey's multiple comparisons test; survival curves were compared using the Log-rank Mantel-Cox test).

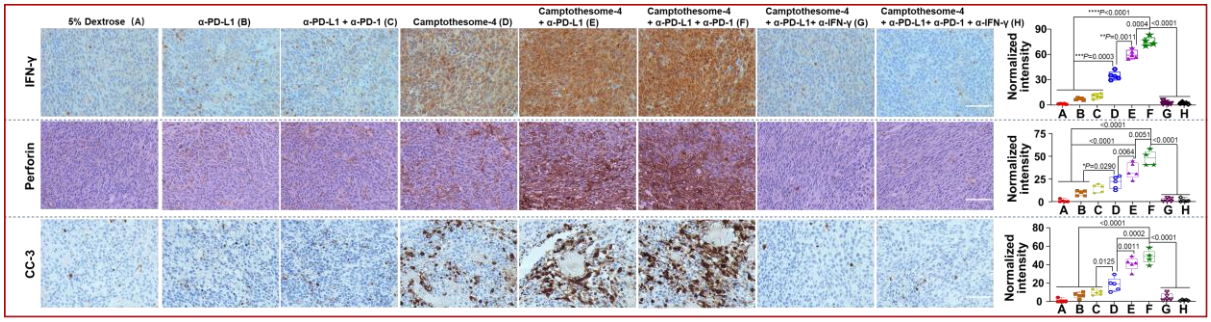

Supplementary Figure 18. Representative IHC staining (scale bar: 100 μm) and normalized intensity compared to vehicle control (5% Dextrose) for IFN-γ, Perforin, and CC-3 in CT26 tumours from **Fig. 4d,e**. Data in (right panel) are expressed as mean ± SD and presented as box-and-whisker plots; boxes delineate lower and upper quartiles of the data; middle lines show median values; dots show individual data points; whiskers show minimal and maximal values for each dataset). [n = 4 (group **F,** one tumour-free mouse) or 5 (other groups) independent mice tumours]. **P* < 0.05, ***P* < 0.01, *****P* < 0.0001 (Statistical significance was determined by one-way ANOVA followed by Tukey's multiple comparisons test).

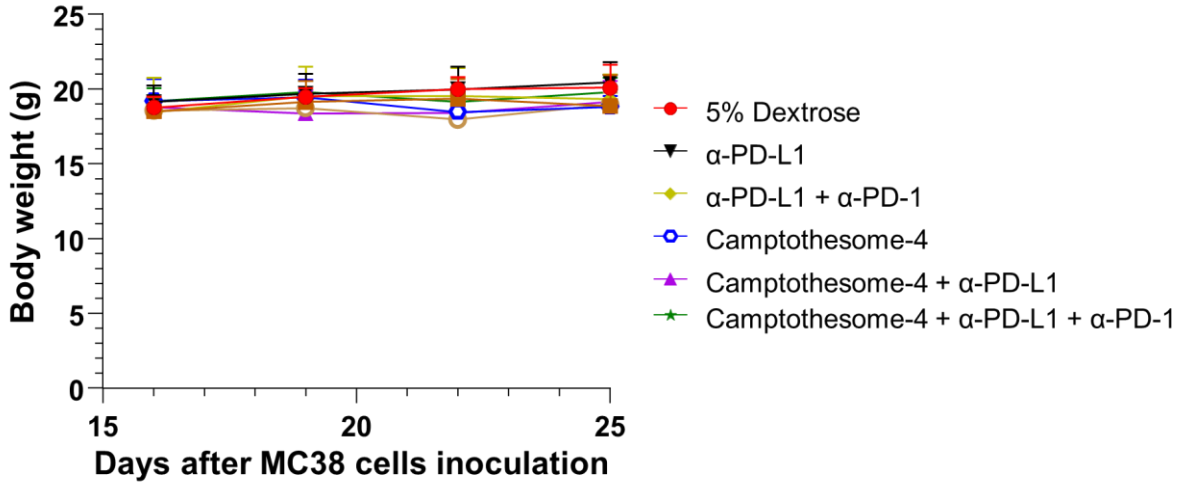

Supplementary Figure 19. Mice body weight in efficacy study presented in **Fig. 4i, j.** Data are represented as mean ± SD (n = 6 mice; one mouse death from 5% Dextrose on day 23).

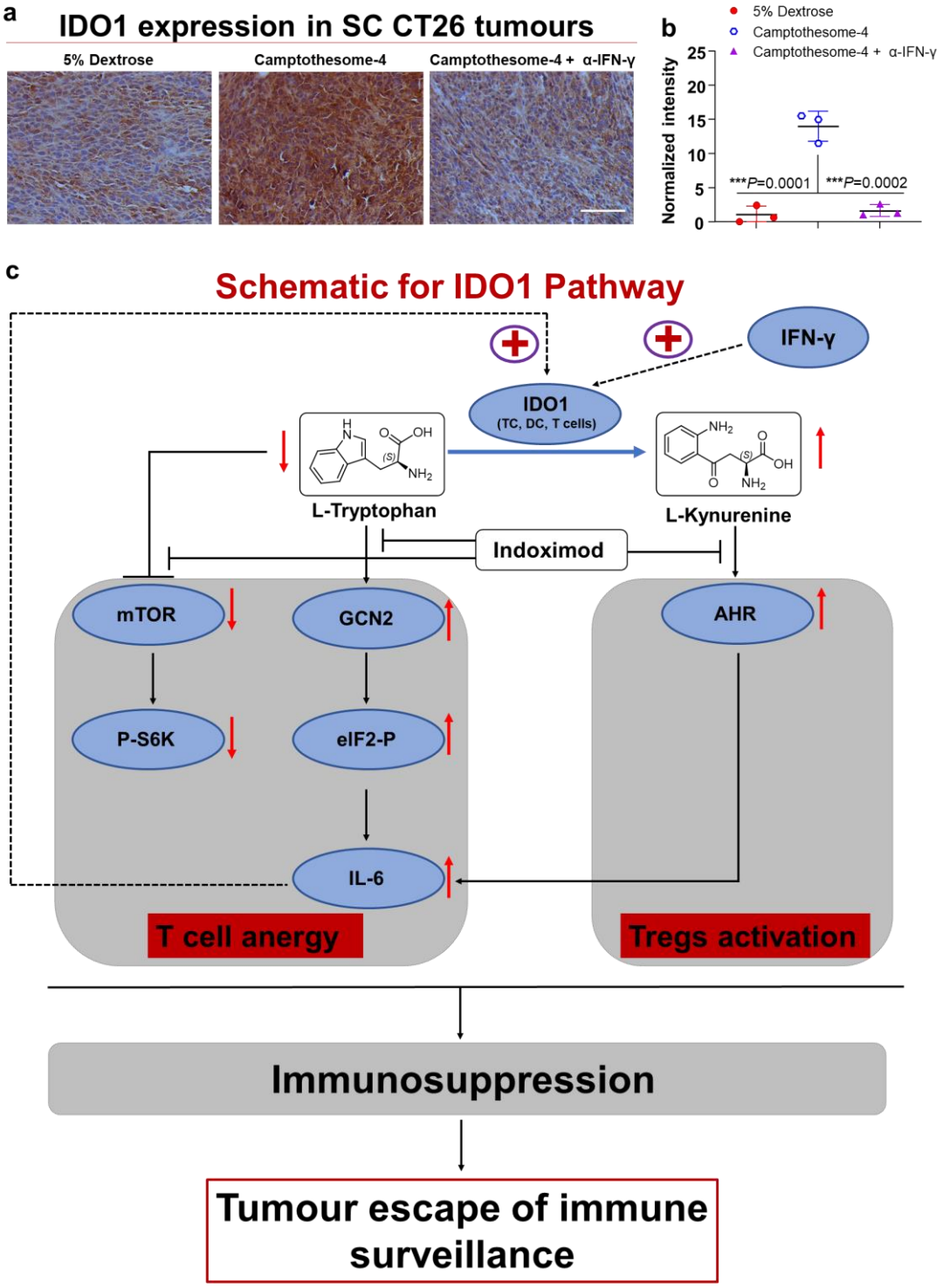

Supplementary Figure 20. a,b, Representative IHC staining (**a**, scale bar: 100 μm) and quantitative analysis (**b**) for IDO1 in CT26 tumours in **Fig. 4d. c**, Schematic for IDO1 pathway entailing the downstream mTOR, GCN2, and AHR signaling. Data in (**b**) are expressed as mean ± SD (n = 3 independent mice tumours). ***P < 0.001 (Statistical significance was determined by one-way ANOVA followed by Tukey's multiple comparisons test).

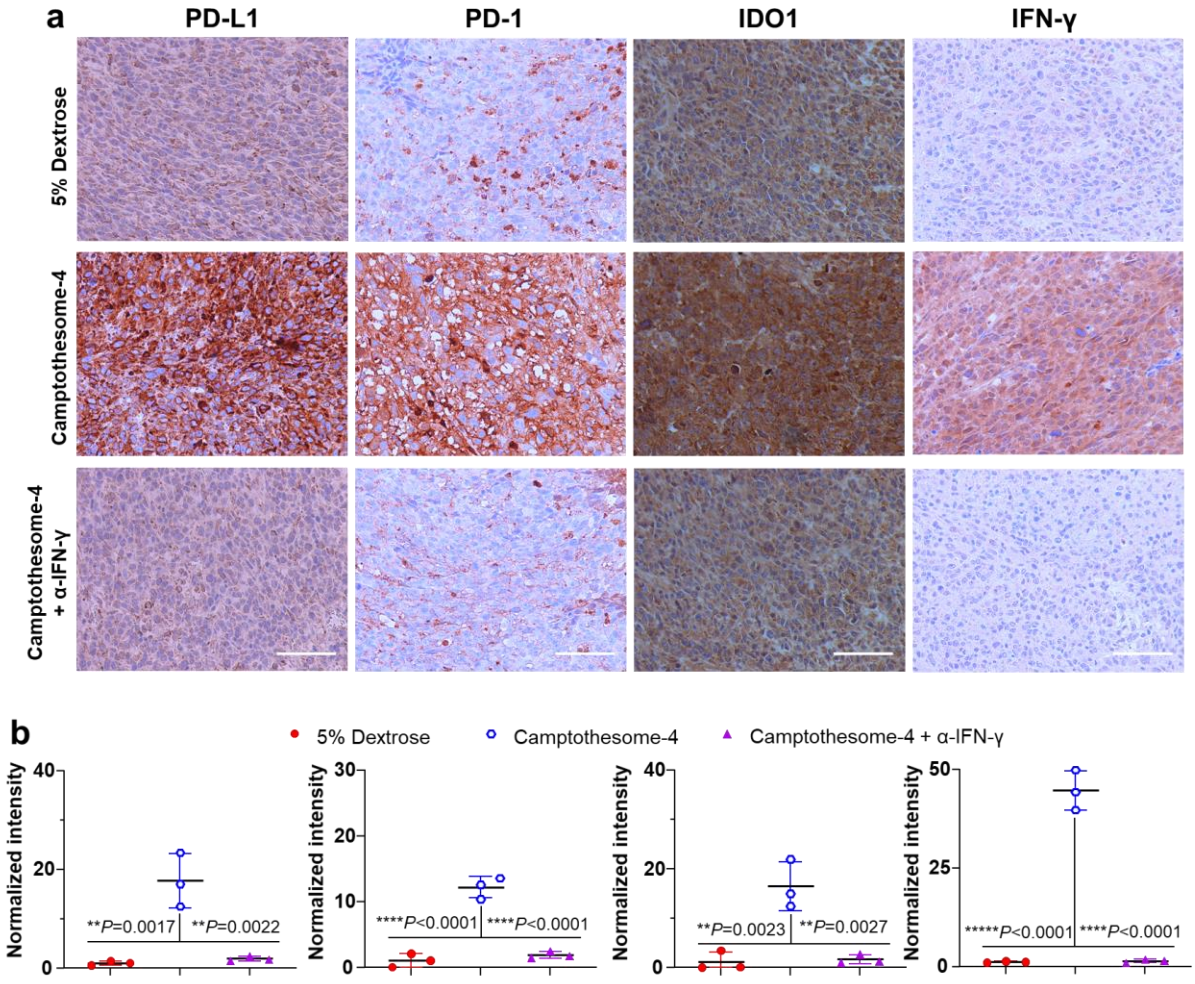

Supplementary Figure 21. Representative IHC staining (**a**) and quantitative analysis (**b**) for PD-L1, PD-1, and IFN-γ in MC38 tumours. Scale bar: 100 μm. SC MC38 tumour-bearing C57BL/6 mice (~200 mm^3) received a single IV injection of Camptothesome-4 (20 mg CPT/kg) and vehicle control. α-IFN-γ was IP injected at 200 μg/mouse/3 days. At day 7 post treatment, tumours were collected and subject to IHC staining for PD-L1, PD-1, and IFN-γ. Data in (**b**) are expressed as mean ± SD (n = 3 independent mice tumours). $^{**}P < 0.01$, $^{****}P < 0.0001$ (Statistical significance was determined by one-way ANOVA followed by Tukey's multiple comparisons test).

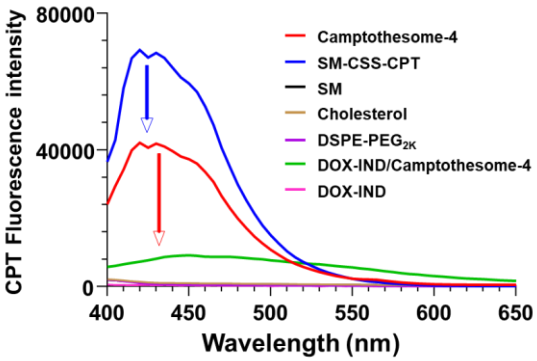

Supplementary Figure 22. CPT fluorescence quenching in Camptothesome-4 and DOX-IND/Camptothesome-4. Experiments were independently repeated for three times.

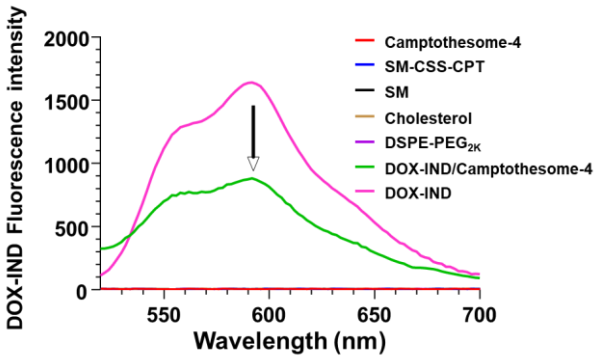

Supplementary Figure 23. DOX-IND fluorescence quenching in Camptothesome-4 and DOX-IND/Camptothesome-4. Experiments were independently repeated for three times.

a

	DOX-IND/ Camptothesome-4	Folate/DOX-IND/ Camptothesome-4	IND/Camptothesome-4
DOX-IND DLC (%)	22.0%±2.4	20.9%±3.3	N/A
IND DLC (%)	5.1%±0.9	4.9%±1.2	<0.5%
DOX DLC(%)	12.8%±1.6	12.1%±2.1	N/A
DLE (%)	83.6%±4.2	80.1%±3.9	29.3%±3.7
DLS size by intensity (d.nm)	100.2±4.13	101.1±3.24	214.1±19.82
Polydispersity index	0.105±0.067	0.096±0.059	0.231±0.091
Zeta potential (mV)	-25.8 ±3.40	-26.7 ±2.11	-20.5±4.59

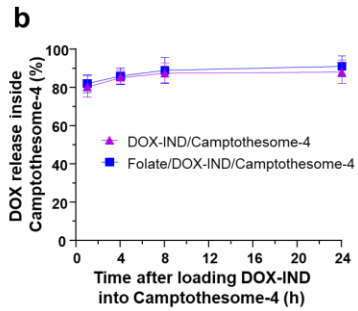

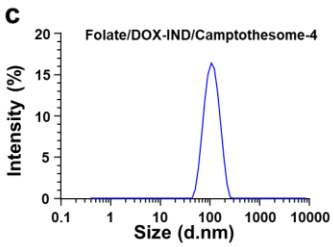

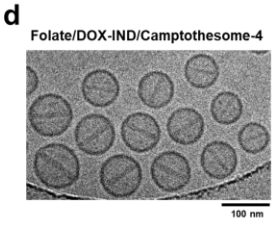

Supplementary Figure 24. Development of DOX-IND-laden Camptothesome-4 with or with folate targeting. **a**, Physicochemical characterizations of DOX-IND/Camptothesome-4, Folate/DOX-IND/Camptothesome-4, and IND/Camptothesome-4. Direct loading of IND to Camptothesome-4 was challenging as evidenced by <0.5% DLC. **b**, DOX release kinetics from DOX-IND inside Camptothesome-4 after remote loading procedure. **c**,**d**, Representative DLS size distribution (**c**) and Cryo-EM (**d**) of Folate/DOX-IND/Camptothesome-4. Data in (**a, b**) are expressed as mean ± SD (n = 3 independent experiments).

a

Formulation	CPT/DOX-IND Dose (mg/kg)	Animal death	Weight loss (%)
DOX-IND/ Camptothesome-4	15/5	0/3	1.16 ± 2.81
	20/6.7	0/3	12.1 ± 1.35
	25/8.3	1/3	N/A
	30/10	2/3	N/A

b

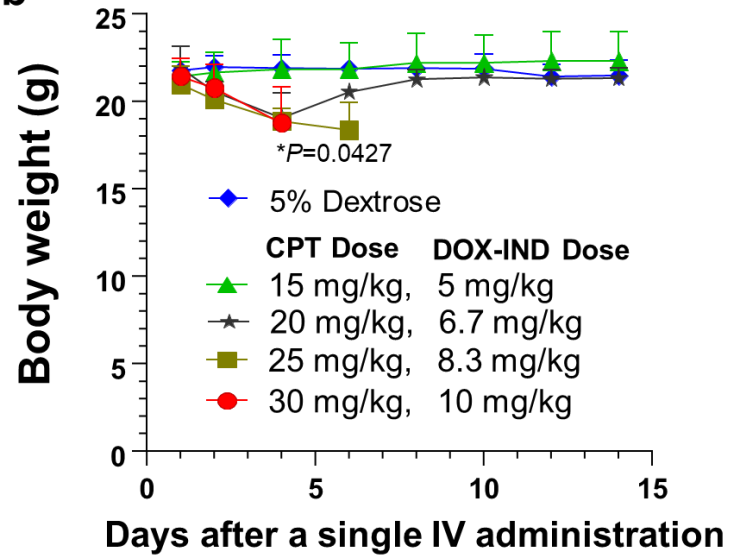

Supplementary Figure 25. MTD Investigation for DOX-IND/Camptothesome-4 (2% of DOX-IND DLC). Data are expressed as mean ± SD (n = 3 mice). **P* = 0.0427 compared to the starting point in 30 mg/kg group in **b** (two-tailed, unpaired Student's *t*-test).

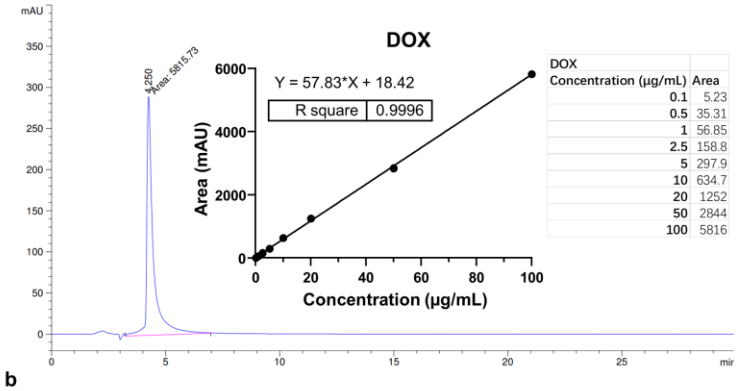

Instrumentation	
HPLC Unit	Agilent 1100 (USA)
Detector	Agilent G1315B Diode-Array Detector
Integrator	Agilent ChemStation Software
Chromatographic conditions	
Column	Waters Symmetry ODS (250mm X 4 mm X 5 µm)
Mobile Phase	ACN : NH_4Ac (15 mM) (60:40 v/v)
Flow Rate	1 mL/min
Injection Volume	50 µL
λ_{max}	470 nm

b

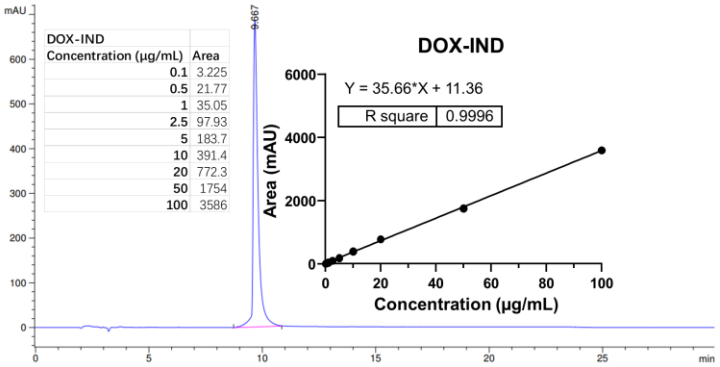

Instrumentation	
HPLC Unit	Agilent 1100 (USA)
Detector	Agilent G1315B Diode-Array Detector
Integrator	Agilent ChemStation Software
Chromatographic conditions	
Column	Waters Symmetry ODS (250mm X 4 mm X 5 µm)
Mobile Phase	ACN : NH_4Ac (15 mM) (60:40 v/v)
Flow Rate	1 mL/min
Injection Volume	50 µL
λ_{max}	470 nm

c

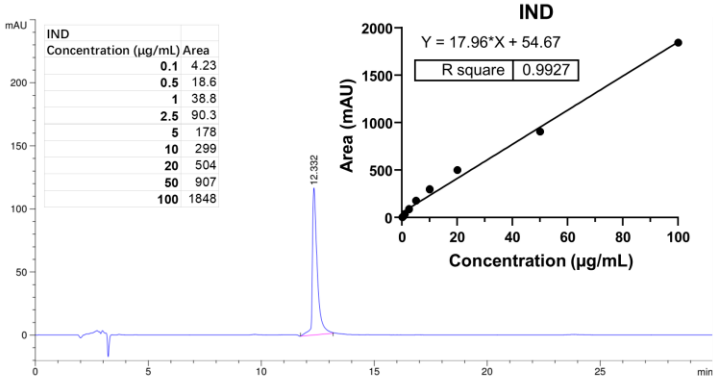

Instrumentation	
HPLC Unit	Agilent 1100 (USA)
Detector	Agilent G1315B Diode-Array Detector
Integrator	Agilent ChemStation Software
Chromatographic conditions	
Column	Waters Symmetry ODS (250mm X 4 mm X 5 µm)
Mobile Phase	ACN : NH_4Ac (15 mM) (60:40 v/v)
Flow Rate	1 mL/min
Injection Volume	50 µL
λ_{max}	254 nm

d

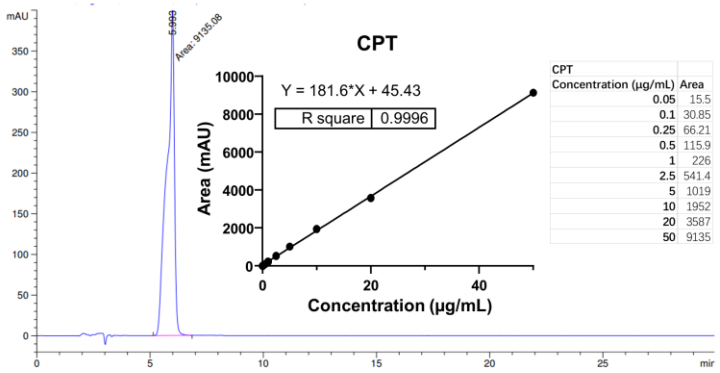

Instrumentation	
HPLC Unit	Agilent 1100 (USA)
Detector	Agilent G1315B Diode-Array Detector
Integrator	Agilent ChemStation Software
Chromatographic conditions	
Column	Waters Symmetry ODS (250mm X 4 mm X 5 µm)
Mobile Phase	ACN : NH_4Ac (15 mM) (60:40 v/v)
Flow Rate	1 mL/min
Injection Volume	50 µL
λ_{max}	370 nm

Supplementary Figure 26. Analytic Reverse-phase HPLC method development for determining the drug concentrations in DOX-IND/Camptothesome-4 and Folate/DOX-IND/Camptothesome-4, and in their pharmacokinetics and biodistribution profiles in orthotopic CT26-Luc CRC murine model. **a-e,** respective representative HPLC chromatogram, standard curve, and HPLC instrumentation and chromatographic conditions for DOX (**a**), DOX-IND (**b**), IND (**c**), CPT (**d**).

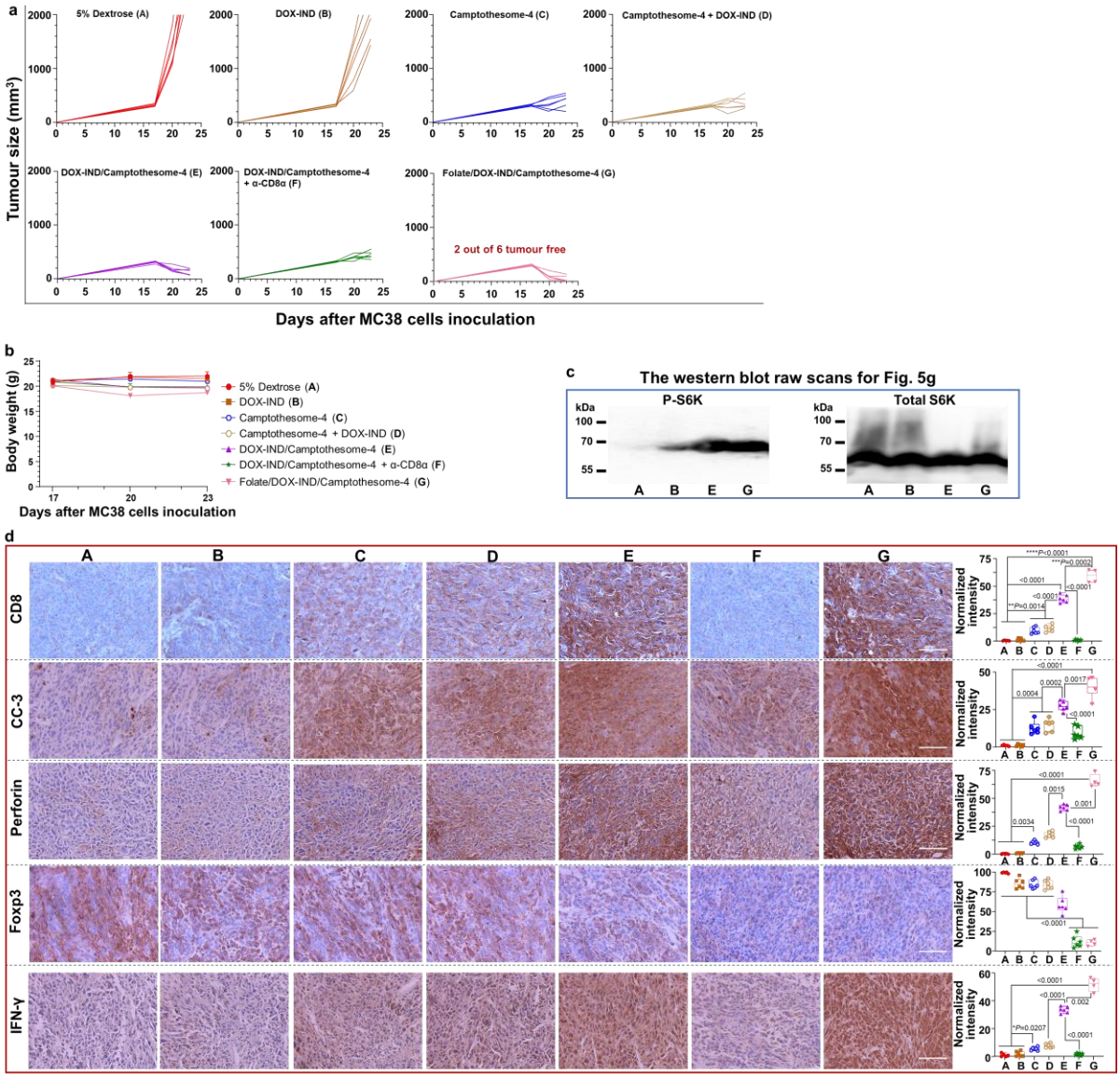

Supplementary Figure 27. Individual tumour growth curves (**a**), mice body weight (**b,** n = 6 mice; on day 22, one mouse died from group **A**), the western blot raw scans (**c**) for Fig. 5g and representative IHC staining for various immune biomarkers and respective quantitative analysis [**d,** n = 5 (group **A)**, 6 (group **B-F)**, or 4 (group **G**, two tumour-free mice) independent mice tumours from the therapeutic efficacy study presented in **Fig 5f, i**]**.** Scale bar: 100 μm. Data in (**b**) are expressed as mean ± SD, and data in (**d**, right panel) are presented as box-and-whisker plots; boxes delineate lower and upper quartiles of the data; middle lines show median values; dots show individual data points; whiskers show minimal and maximal values for each dataset. **P* < 0.05, ***P* < 0.01, ****P* < 0.001, *****P* < 0.0001 (Statistical significance was determined by one-way ANOVA followed by Tukey's multiple comparisons test).

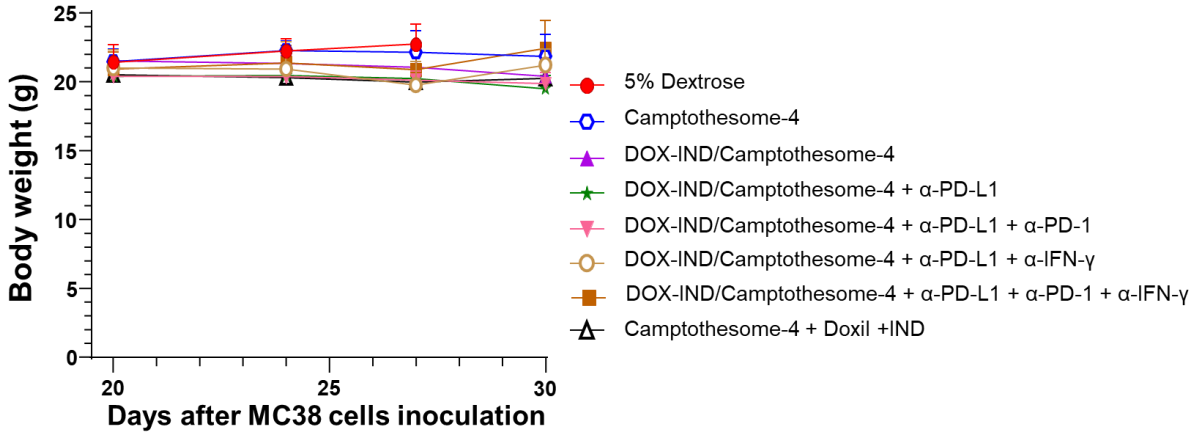

Supplementary Figure 28. Mice body weight change over time from the anticancer efficacy investigation displayed in **Fig 5k-m.** Data are presented as mean ± SD (n = 5 mice; one mouse death from vehicle control on day 21).

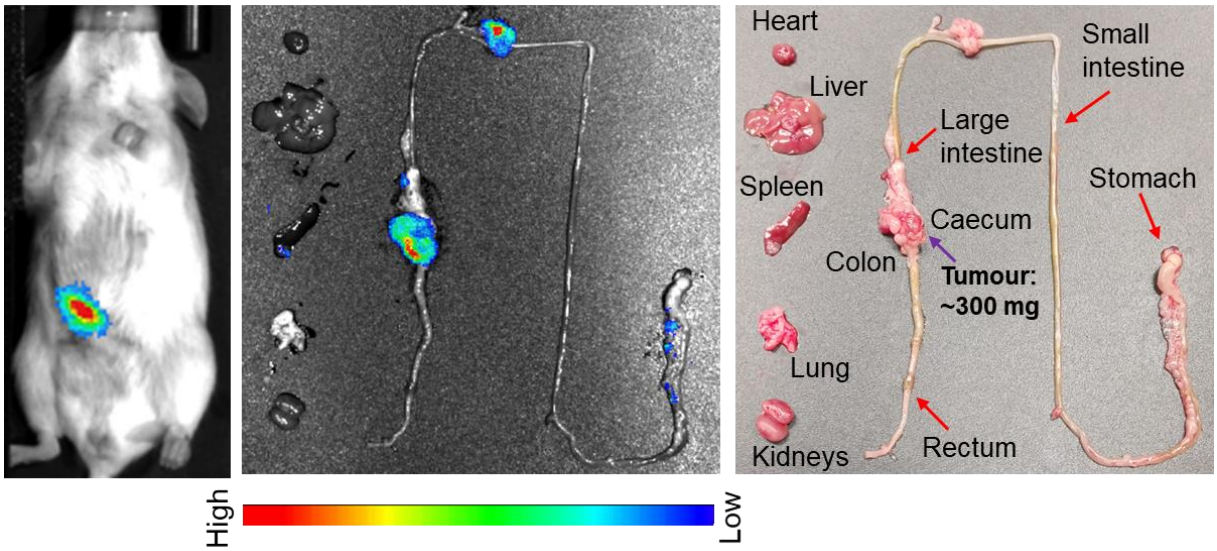

Supplementary Figure 29. Representative *ex vivo* Lago bioluminescence imaging (left panel) and photographs (right panel) for various tissues in orthotopic CRC murine model on day 8 post injecting 2 × 10^6 CT26-Luc cells into the caecum subserosa. Experiments were independently repeated for three times.

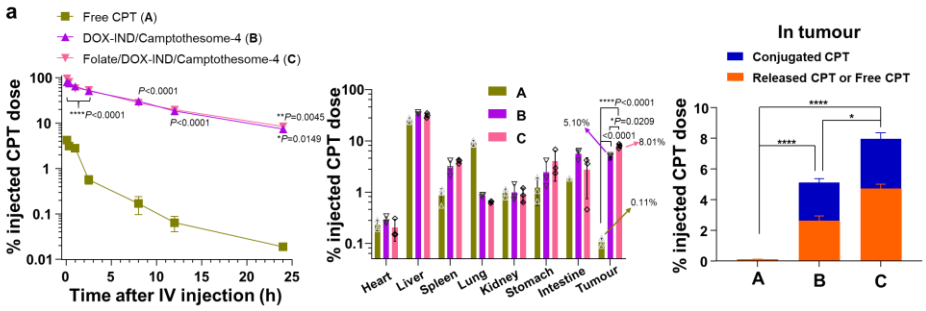

	Free CPT	DOX-IND/Camptothesome-4	Folate/DOX-IND/Camptothesome-4
$T_{1/2}$ (h)	0.06 ± 0.01	5.60 ± 0.68	4.64 ± 0.25
V ((μg)/(μg/ml))	0.77 ± 0.23	1.29 ± 0.10	1.17 ± 0.02
CL(μg)/(μg/ml)/h)	10.62 ± 1.00	0.16 ± 0.01	0.18 ± 0.01
AUC_{0-t} (μg/ml*h)	9.47 ± 0.87	2365.19 ± 166.45	2225.37 ± 111.96
AUC_{0-inf} (μg/ml*h)	9.48 ± 0.88	2497.07 ± 214.81	2289.75 ± 126.47
AUMC (μg/ml*h^2)	8.12 ± 0.38	20279.95 ± 4095.06	15365.22 ± 1623.18
MRT (h)	0.86 ± 0.04	8.07 ± 0.98	6.70 ± 0.35
V_{ss} (μg/(μg/ml))	9.16 ± 1.30	1.29 ± 0.10	1.17 ± 0.02

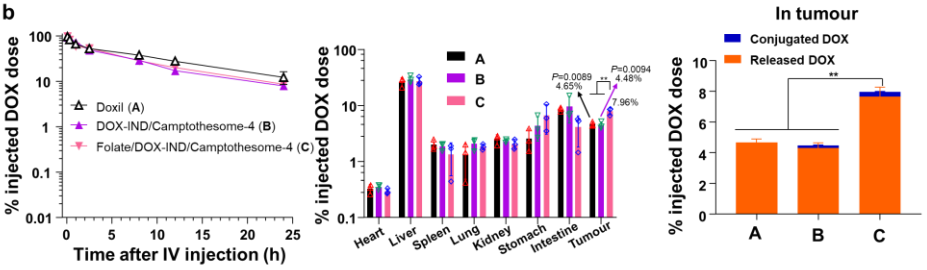

	Doxil	DOX-IND/Camptothesome-4	Folate/DOX-IND/Camptothesome-4
$T_{1/2}$ (h)	4.01 ± 0.23	3.24 ± 0.99	3.03 ± 0.86
V ((μg)/(μg/ml))	1.19 ± 0.01	1.12 ± 0.08	1.11 ± 0.04
CL(μg)/(μg/ml)/h)	0.13 ± 0.01	0.18 ± 0.03	0.19 ± 0.03
AUC_{0-t} (μg/ml*h)	587.89 ± 15.88	432.03 ± 57.66	436.79 ± 65.96
AUC_{0-inf} (μg/ml*h)	639.74 ± 22.20	443.70 ± 69.18	448.19 ± 75.28
AUMC (μg/ml*h^2)	6108.87 ± 428.73	2844.68 ± 1118.33	2868.49 ± 1037.24
MRT (h)	9.54 ± 0.34	6.26 ± 1.43	6.26 ± 1.24
V_{ss} (μg/(μg/ml))	1.19 ± 0.01	1.12 ± 0.08	1.11 ± 0.04

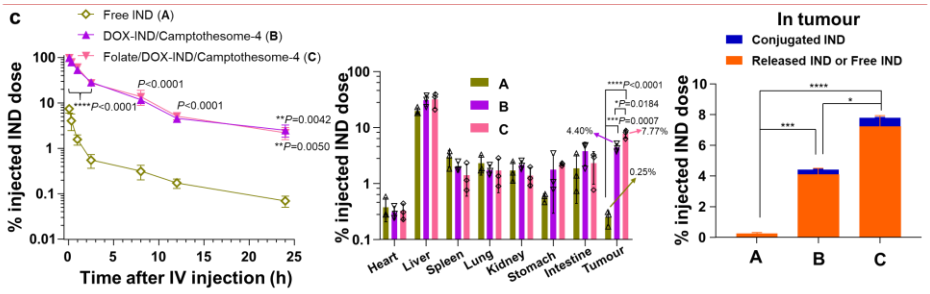

	Free IND	DOX-IND/Camptothesome-4	Folate/DOX-IND/Camptothesome-4
$T_{1/2}$ (h)	0.08 ± 0.02	2.32 ± 0.05	2.48 ± 0.08
V ((μg)/(μg/ml))	4.94 ± 0.63	1.07 ± 0.04	1.06 ± 0.03
CL(μg)/(μg/ml)/h)	12.08 ± 1.17	0.53 ± 0.01	0.52 ± 0.02
AUC_{0-t} (μg/ml*h)	5.66 ± 0.53	59.64 ± 1.36	65.08 ± 2.73
AUC_{0-inf} (μg/ml*h)	5.67 ± 0.54	59.65 ± 1.37	65.09 ± 2.74
AUMC (μg/ml*h^2)	2.38 ± 0.71	112.51 ± 5.71	132.27 ± 11.64
MRT (h)	0.41 ± 0.09	1.88 ± 0.07	2.03 ± 0.11
V_{ss} (μg/(μg/ml))	4.95 ± 0.63	1.07 ± 0.03	1.06 ± 0.03

Supplementary Figure 30. Pharmacokinetics and biodistribution in orthotopic CRC murine model. 2 × 10^6 CT26-Luc cells were injected in the caecum subserosa of BALB/c mice. 8 days later, mice were IV administered once by Doxil, free CPT, DOX-IND/Camptothesome-4, or Folate/DOX-IND/Camptothesome-4 at eq. 20 CPT/kg, 1.7 mg IND/kg or 4 mg DOX/kg. Blood

kinetics, tissue distribution, intratumoural drug release and pharmacokinetic parameter of CPT (**a**), DOX (**b**) and IND (**c**). Data are expressed as mean ± SD (n = 3 mice). *P < 0.05, **P < 0.01, ***P < 0.001, ****P < 0.0001 (Statistical significance was determined by one-way ANOVA followed by Tukey's multiple comparisons test).

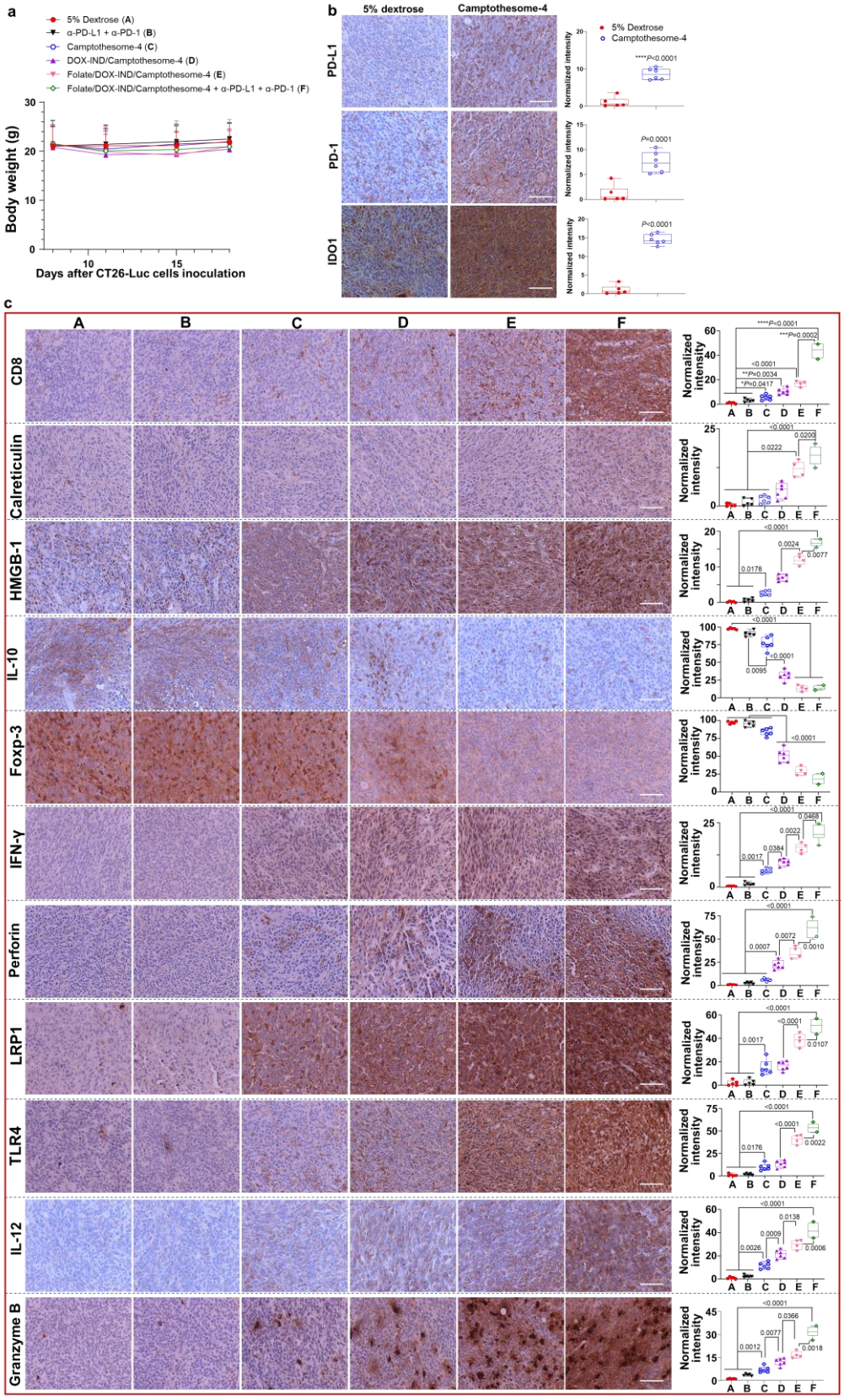

Supplementary Figure 31. Mice body weight (**a**, n = 6 mice; one mouse died from groups **A** and **B** on day 18) and representative IHC staining for PD-L1, PD-1, and IDO1 (**b**), and various other immune biomarkers (**c**) and respective quantitative analysis [n = 5 (groups **A,B**), 6

(groups **C,D**), 4 (group **E**; 2 tumour-free mice), 2 (group **F**; 4 tumour-free mice) independent mice tumours] from efficacy study shown in **Fig. 6a,b.** Scale bar (b,c): 100 μm. Data in (**a**) are expressed as mean ± SD, and data in (**b**, **c,** right panel) are presented as box-and-whisker plots; boxes delineate lower and upper quartiles of the data; middle lines show median values; dots show individual data points; whiskers show minimal and maximal values for each dataset. **P* < 0.05, ***P* < 0.01, ****P* < 0.001, *****P* < 0.0001 (two-tailed, unpaired Student's *t*-test for **b;** Statistical significance was determined by one-way ANOVA followed by Tukey's multiple comparisons test for **c**).

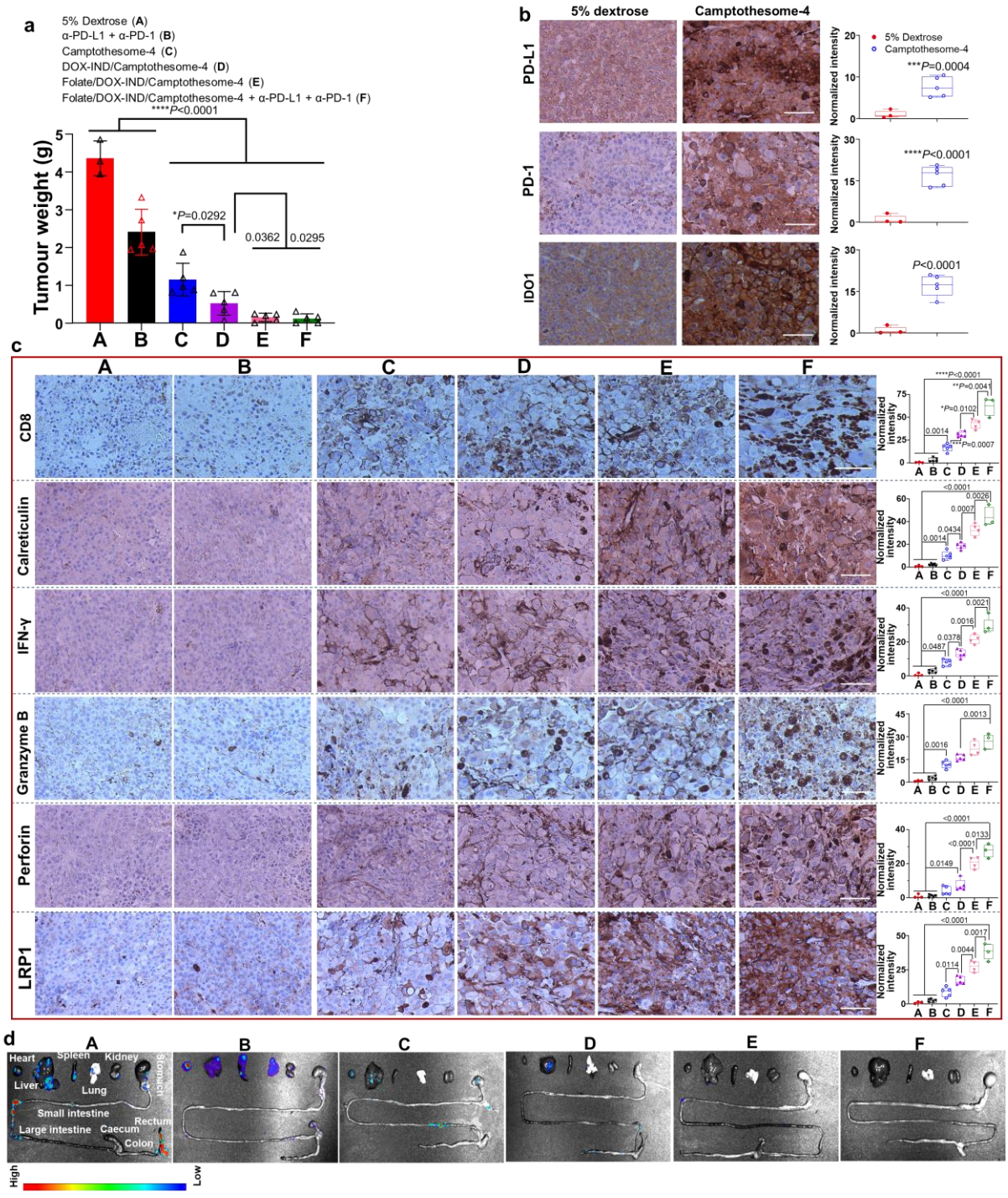

Supplementary Figure 32. Tumour weight (**a**, group **E** and **F** have 1 and 2 tumour-free mice, respectively; hence the tumour weight for these mice is "0") and representative IHC for PD-L1, PD-1 and IDO1 (**b**), and CD8, Calreticulin, IFN-γ, Granzyme B, Perforin and LRP1(**c**), and respective quantitative analysis [n = 3 (group **A,** 2 mice death), 5 (groups **B-D**), 4 (group **E**, 1 tumour-free mouse), or 3 (group **F**, 2 tumour-free mice) independent mice tumours); representative *ex vivo* bioluminescence imaging in various organs (**d**) in SC melanoma tumours from therapeutic efficacy study in **Fig. 6f-i.** Scale bar (**b, c**): 100 μm. Data in (**a**) are expressed as mean ± SD, and data in (**b, c**, right panel) are presented as box-and-whisker

plots; boxes delineate lower and upper quartiles of the data; middle lines show median values; dots show individual data points; whiskers show minimal and maximal values for each dataset. *P < 0.05, **P < 0.01, ***P < 0.001, ****P < 0.0001 (Statistical significance was determined by one-way ANOVA followed by Tukey's multiple comparisons test for **a**,**c;** two-tailed, unpaired Student's *t*-test for **b**).

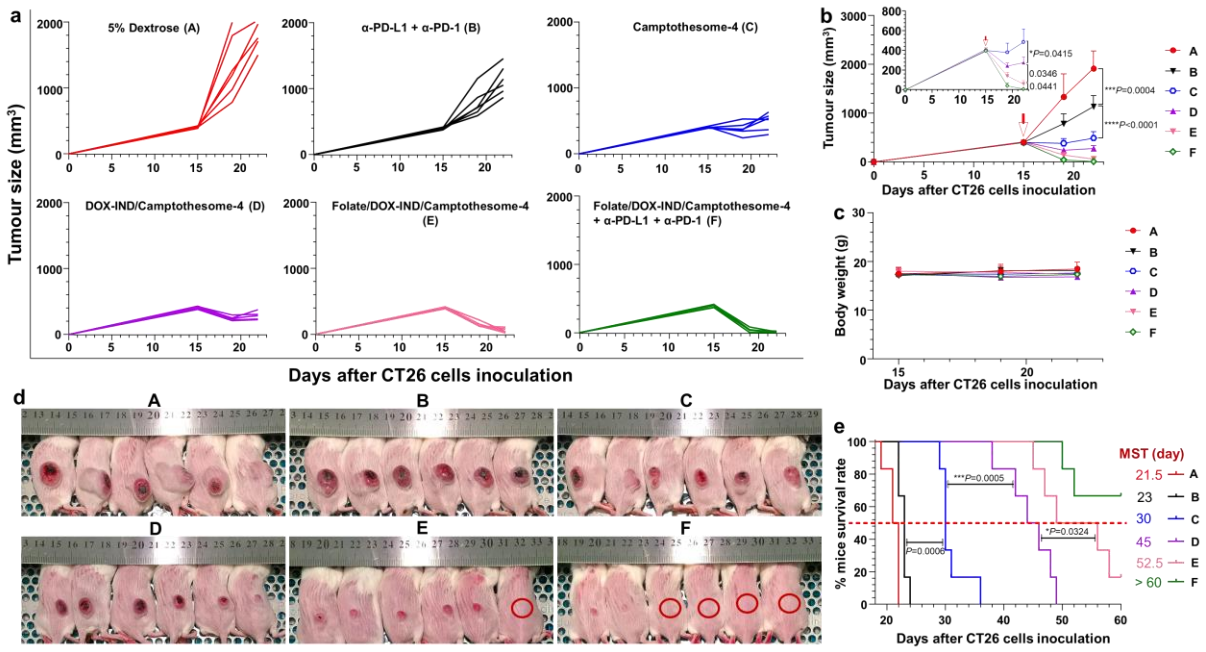

Supplementary Figure 33. Antitumour efficacy in SC CT26 tumour murine model. On day 15, when tumours were ~400 mm^3, mice (n = 6) were IV administered once by eq. 15 mg CPT/kg (5 mg DOX-IND/kg). α-PD-L1 and α-PD-1 were IP injected (100 µg/mouse) from day 12 every 3 days for 3 times. **a**, Individual tumour growth curves. **b**, Average tumour growth curves. **c**, Mice body weight. **d**, tumour-bearing mice images taken on day 22. Red circle means tumour-free mouse. **e**, Kaplan–Meier survival curves. Data in (**b, c**) are represented as mean ± SD. *P < 0.05, ***P < 0.001, ****P < 0.0001 (Statistical significance was determined by one-way ANOVA followed by Tukey's multiple comparisons test; survival curves were compared using the Log-rank Mantel-Cox test).

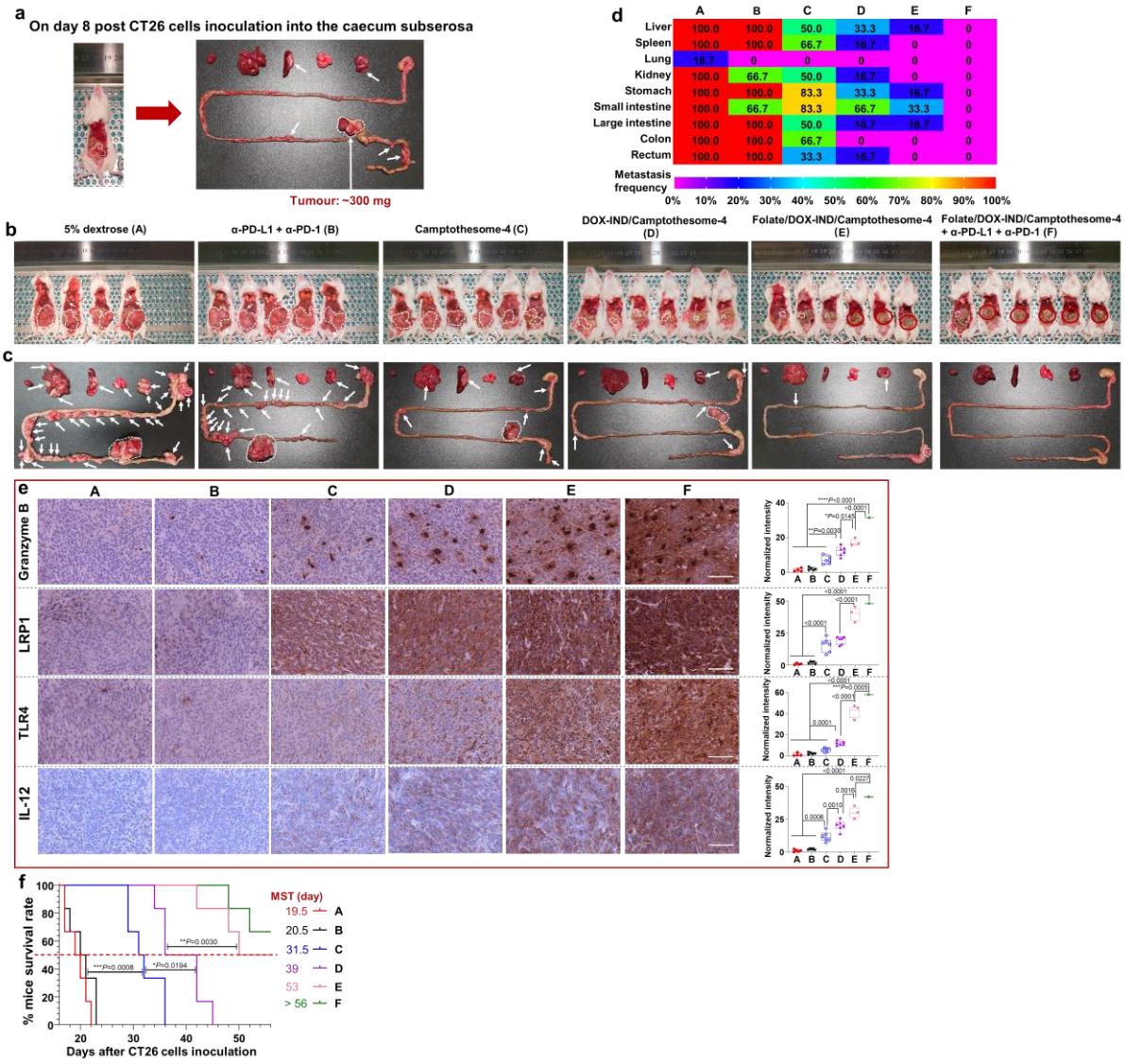

Supplementary Figure 34. a, Representative photographs of mouse and various tissues *ex vivo* in orthotopic CT26 tumour mouse model on day 8 after injecting 2 × 10^6 CT26 cells into the caecum subserosa. **b**, Mice images taken on day 18 after mice (n= 6 mice; tumours: ~300 mg) were administered by various treatments as used in **Fig. 6** on day 8. 2 mice died on day 17 from vehicle control group; 1 mouse died on day 16 from α-PD-L1 + α-PD-1 group. The abdomen of mice was opened to show the tumours. The white dashed circle: big tumour blocks; the white arrow: visible tumour metastatic nodules; red circle: tumour-free mouse. **c**, Representative photograph of various organs *ex vivo*. The white dashed circle: primary tumour; the white arrow: tumour metastatic nodules. **d**, The heatmap exhibiting the tumour metastatic rate for different organs. **e,** Representative IHC staining for Granzyme B, LRP1, TLR4, and IL-12 (**f**), and respective quantitative analysis [n = 4 (group A, 2 mice death), 5 (group B, 1 mouse death), 6 (groups C-D), 3 (group E, 3 tumour-free mice), 1 (group F, 5 tumour-free mice) independent mice tumours in (**b**) on day 18]. Scale bar=100 μm. **f**, Kaplan–Meier survival

curves from a separate efficacy study in orthotopic CT26 tumour model (n = 6 mice; tumours: ~300 mg). Data in (**e**, right panel) are presented as box-and-whisker plots; boxes delineate lower and upper quartiles of the data; middle lines show median values; dots show individual data points; whiskers show minimal and maximal values for each dataset. *P < 0.05, **P < 0.01, ***P < 0.001, ****P < 0.0001 (Statistical significance was determined by one-way ANOVA followed by Tukey's multiple comparisons test; survival curves were compared using the Log-rank Mantel-Cox test).

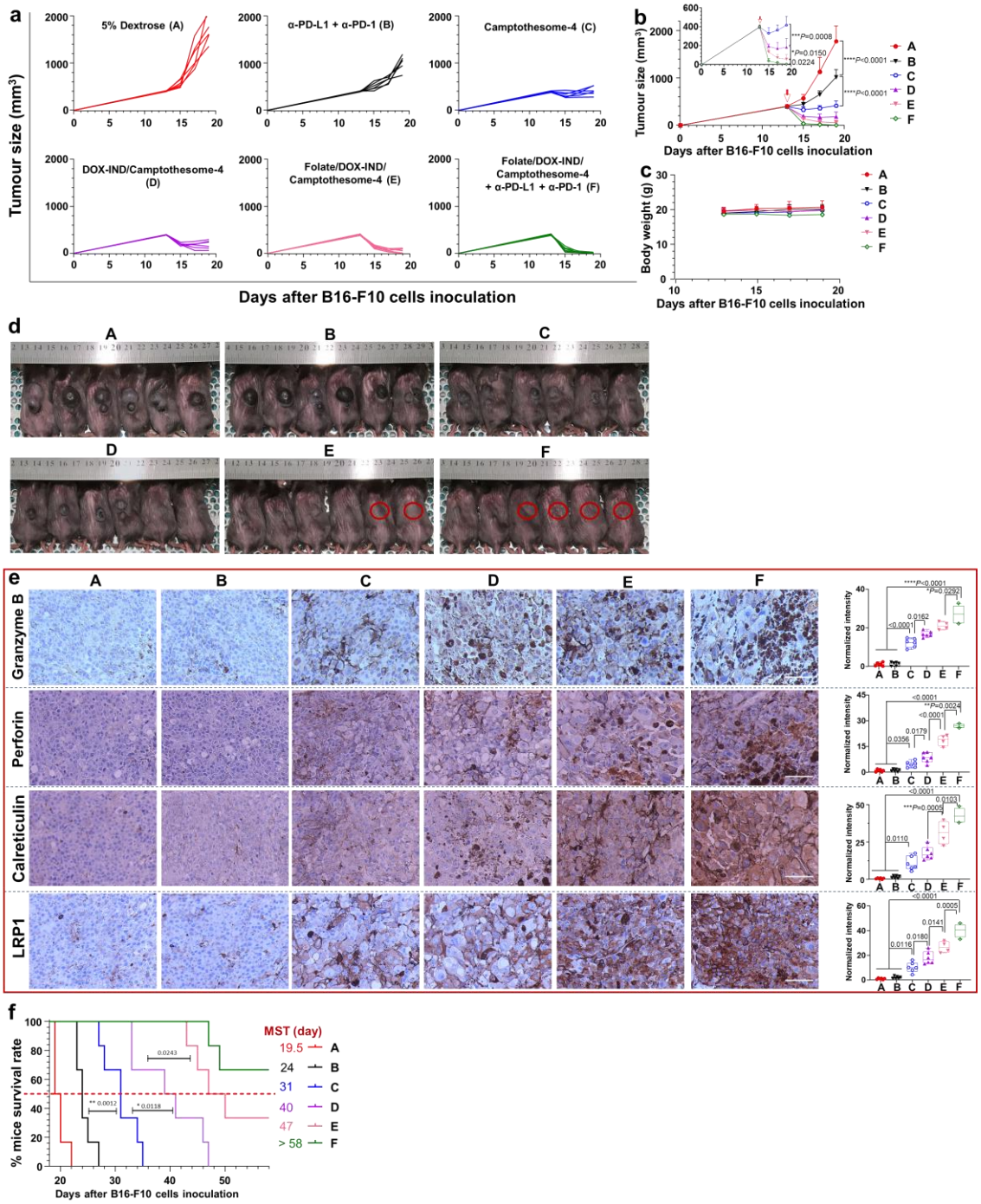

Supplementary Figure 35. Antitumour efficacy in B16-F10 melanoma-bearing C57BL/6 mice. Animals were SC inoculated with 0.1 × 10^6 B16-F10 cells. On day 13, mice (n=6 mice; tumours: ~400 mm^3) received the same treatments as used in **Fig. 6**. **a**, Individual tumour growth curves. **b**, Average tumour growth curves. **c**, Mice body weight. **d**, Tumour-bearing mice images taken on day 19. Red circle means Tumour-free mouse. **e,** Representative IHC staining for Granzyme B, Perforin, Calreticulin, and LRP1 (**f**, scale bar: 100 μm), and respective quantitative analysis [n = 6 (groups A-D), 4 (group E, 2 tumour-free mice), 2 (group F, 4 tumour-free mice) independent mice tumours in (b) on day 19]. **f**, Kaplan–Meier survival curves from a separate efficacy study in B16-F10 tumour model (n = 6 mice; tumours: ~400

mm^3). Data in (**b**, **c**) are represented as mean ± SD, and data in (**e**, right panel) are presented as box-and-whisker plots; boxes delineate lower and upper quartiles of the data; middle lines show median values; dots show individual data points; whiskers show minimal and maximal values for each dataset. *P < 0.05, **P < 0.01, ***P < 0.001, ****P < 0.0001 (Statistical significance was determined by one-way ANOVA followed by Tukey's multiple comparisons test; survival curves were compared using the Log-rank Mantel-Cox test).

Supplementary References

1. Kim SH, *et al.* The self-assembly of anticancer camptothecin-dipeptide nanotubes: a minimalistic and high drug loading approach to increased efficacy. *Chem. - Eur. J.*, **21,** 101-105 (2015).

2. Zhang F, *et al.* Transformative Nanomedicine of an Amphiphilic Camptothecin Prodrug for Long Circulation and High Tumor Uptake in Cancer Therapy. *ACS Nano,* **11,** 8838-8848 (2017).

3. Awuah SG, Zheng YR, Bruno PM, Hemann MT, Lippard SJ. A Pt(IV) Pro-drug Preferentially Targets Indoleamine-2,3-dioxygenase, Providing Enhanced Ovarian Cancer Immuno-Chemotherapy. *J. Am. Chem. Soc.*, **137,** 14854-14857 (2015).

4. Lau UY, *et al.* Lactone Stabilization is Not a Necessary Feature for Antibody Conjugates of Camptothecins. *Mol. Pharmaceutics,* **15,** 4063-4072 (2018).

5. Cheng J, Khin KT, Jensen GS, Liu A, Davis ME. Synthesis of linear, beta-cyclodextrin-based polymers and their camptothecin conjugates. *Bioconjug. Chem.*, **14,** 1007-1017 (2003).

6. Fox ME, *et al.* Synthesis and in vivo antitumor efficacy of PEGylated poly(l-lysine) dendrimer-camptothecin conjugates. *Mol. Pharmacol.*, **6,** 1562-1572 (2009).

7. Crowe AR, Yue W. Semi-quantitative Determination of Protein Expression using Immunohistochemistry Staining and Analysis: An Integrated Protocol. *Bio. Protoc.*, **9,** (2019).